Support vector machine classification of strong gravitational lenses

Philippa Hartley
Jodrell Bank Centre for Astrophysics

+ Rémi Flamary, Neal Jackson, Amit Tagore, Ben Metcalfe

Tuesday Dec 19th 2017, Laboratoire Lagrange, Université Côte d'Azur

The University of Manchester

Overview

- **Lensing overview**
  - Lensing history
  - Types of gravitational lensing
- **Science from strong lenses**
  - Current applications of lenses
  - Euclid sky survey: more lenses
- **An automatic lens finder**
  - Support vector machine approach
- **Application of the lens finder**
  - Lens finding challenge
  - Kilo Degree Survey
- **The future….**

1704: Newton suspects gravitational deflection of light

"Do not bodies act upon light at a distance, and by their action bend its Rays; and is not this action strongest at the least distance ?", *Opticks*

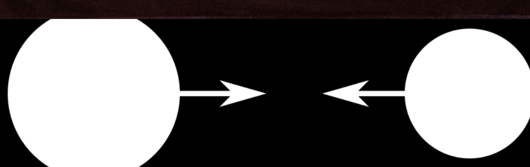

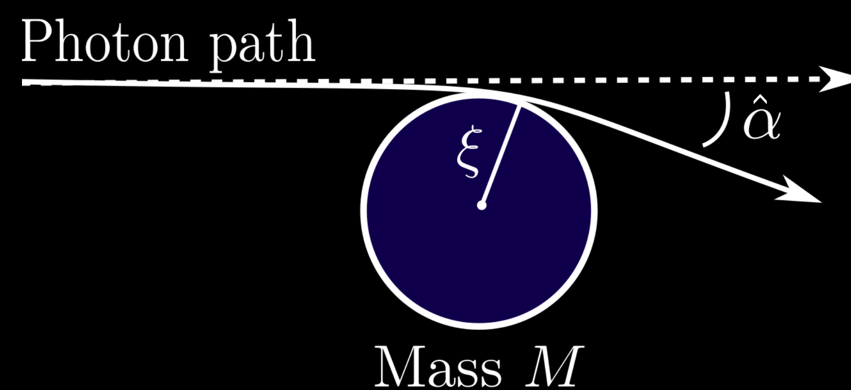

$$\hat{\alpha} = \frac{2GM}{c^2 \xi}$$ J. Soldner, 1804

The University of Manchester

1915: General relativity predicts twice the deflection

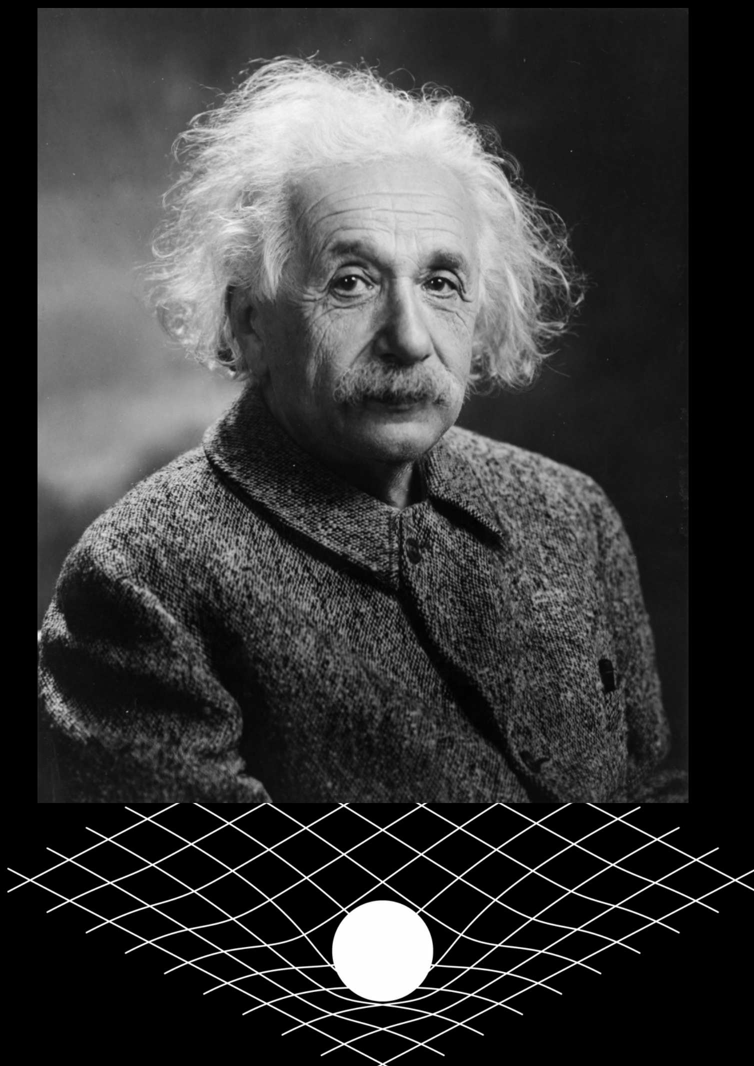

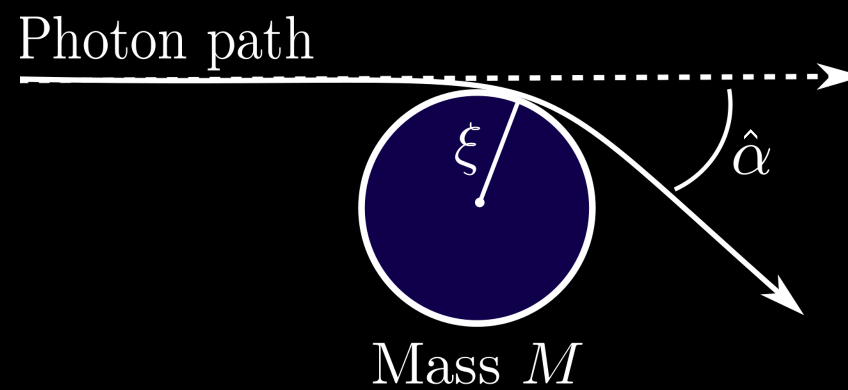

$$\hat{\alpha} = \frac{4GM}{c^2\xi}$$

1919: Lensing effect observed by Arthur Eddington

GR confirmed

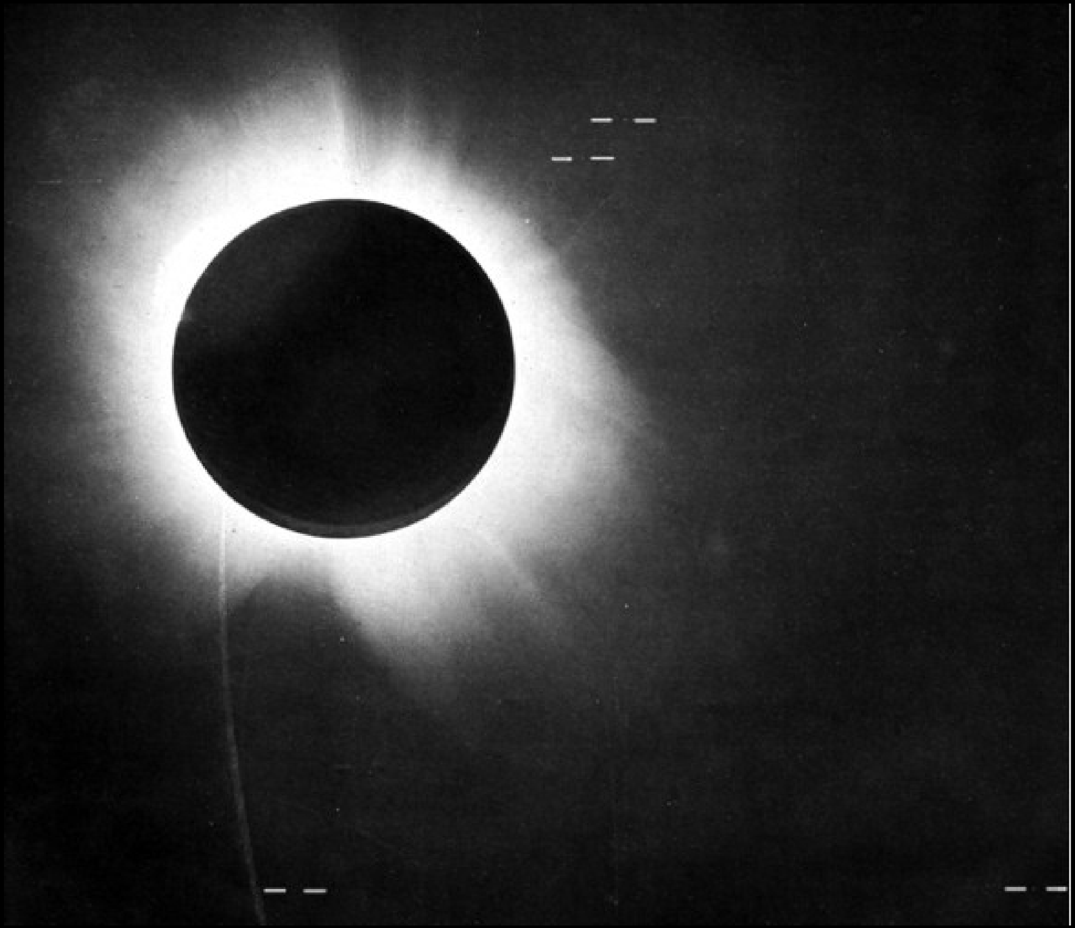

Solar eclipse of 1919, shifted star locations marked

MANCHESTER 1824
The University of Manchester

Lensing formalism

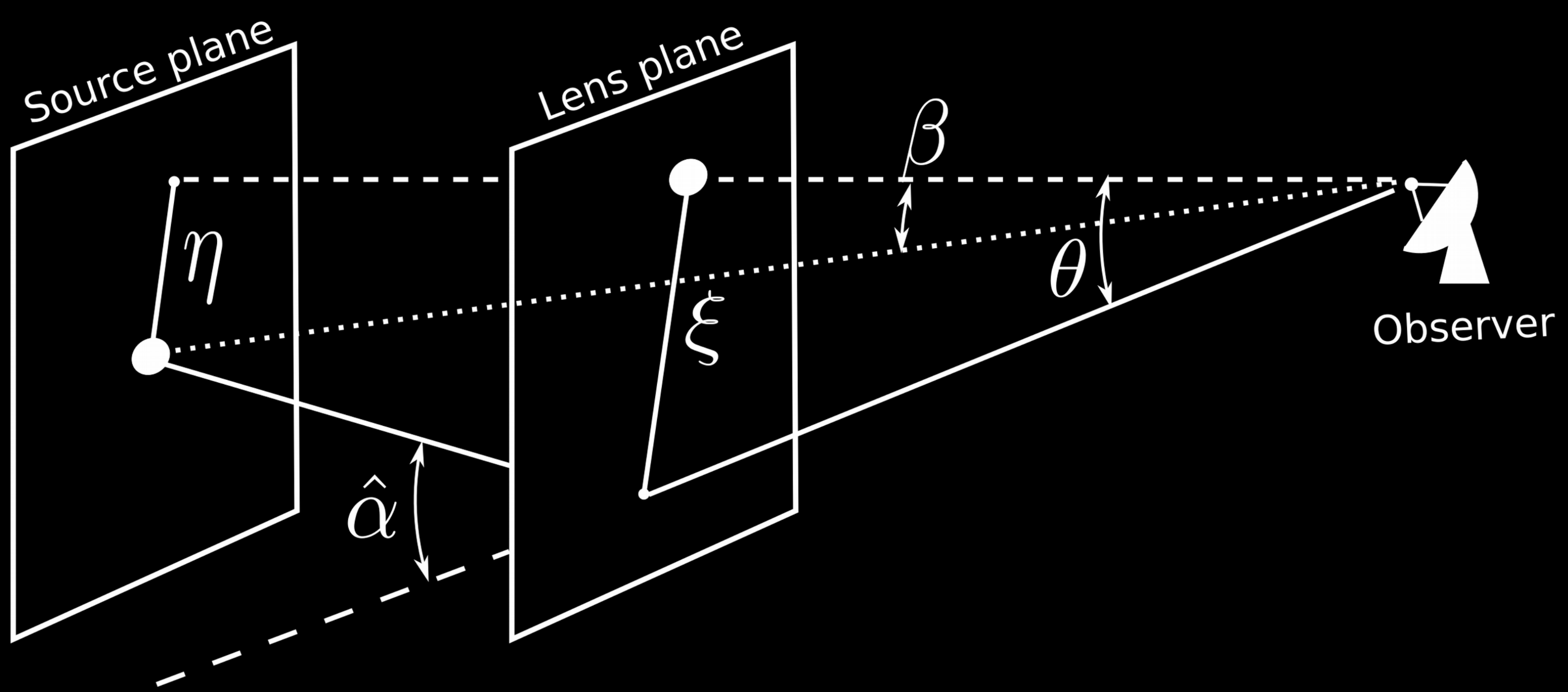

$$\mathcal{A}(\theta) = \frac{\partial \beta}{\partial \theta}$$

Lensing formalism

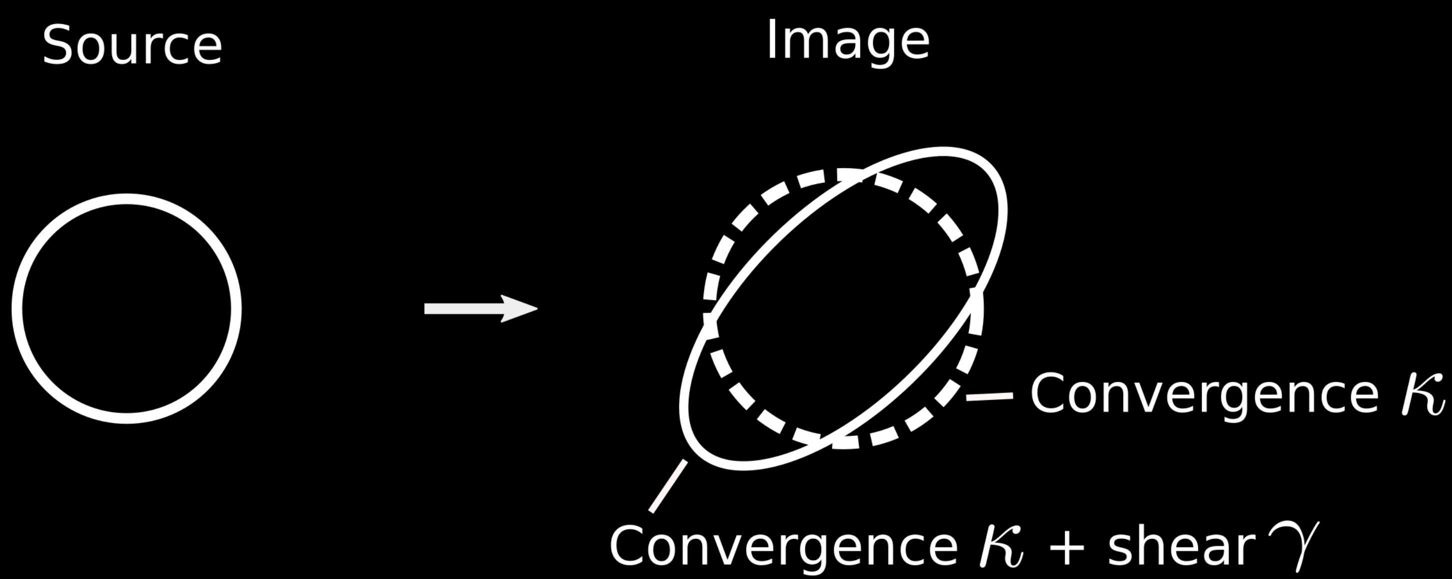

$$\mathcal{A}(\theta) = \frac{\partial \beta}{\partial \theta} = \begin{pmatrix} 1-\kappa-\gamma_1 & \gamma_2 \\ -\gamma_2 & 1-\kappa+\gamma_1 \end{pmatrix}$$

Lensing formalism

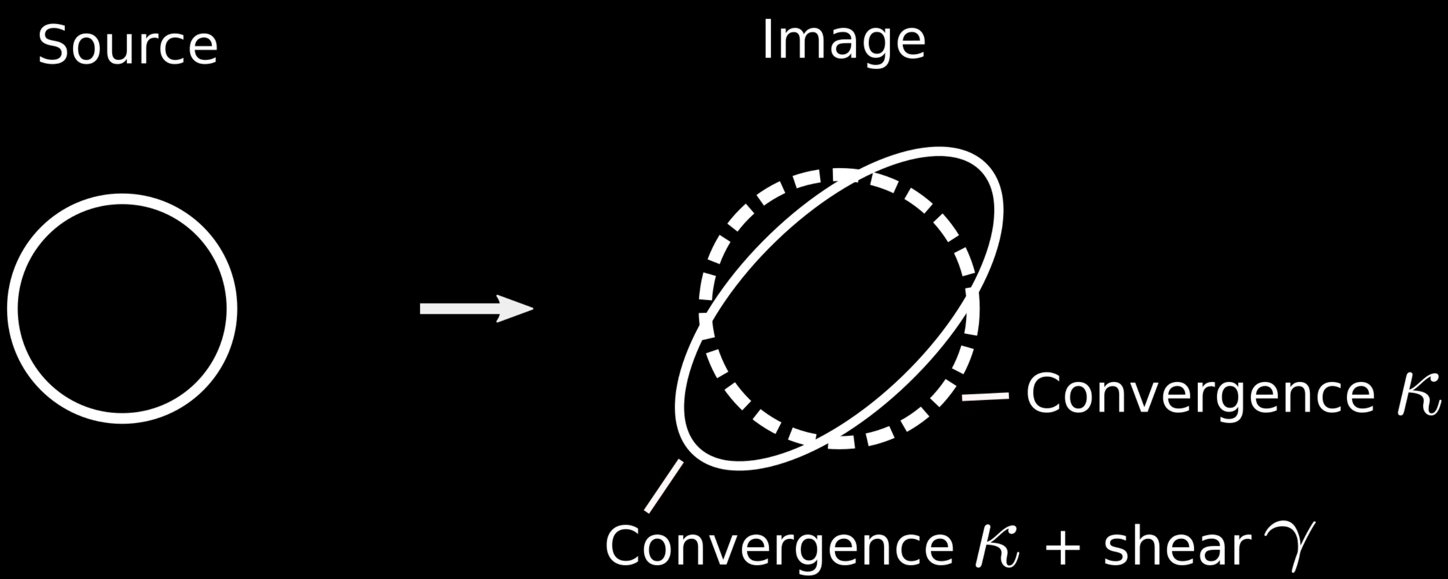

$$\mathcal{A}(\theta) = \frac{\partial \beta}{\partial \theta} = \begin{pmatrix} 1-\kappa-\gamma_1 & \gamma_2 \\ -\gamma_2 & 1-\kappa+\gamma_1 \end{pmatrix};$$ Magnification $\mu = \frac{1}{\det \mathcal{A}}$

Lensing geometry

Cusp configuration

Fold configuration

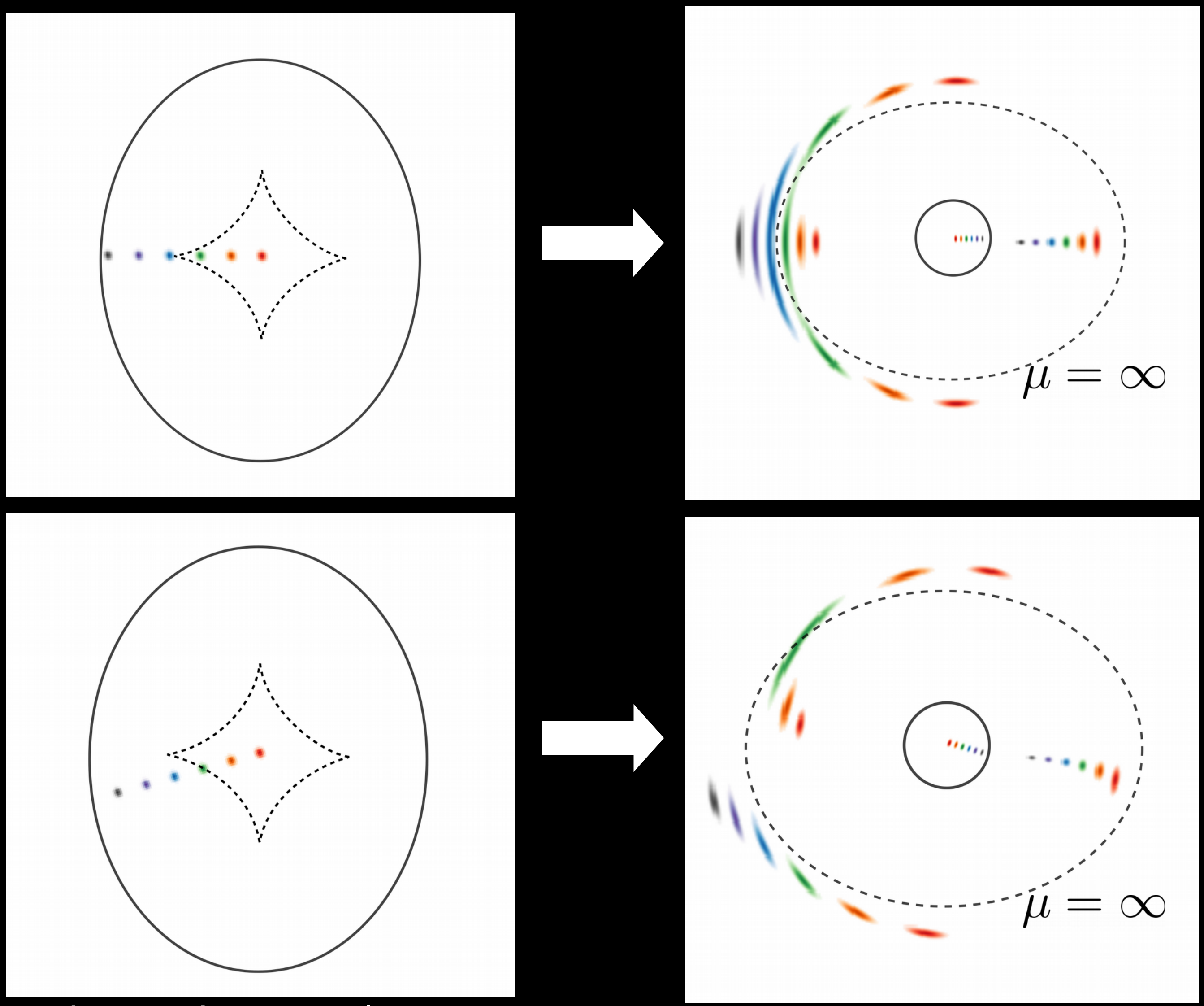

Background source plane

Image plane

Lensing formalism: Fermat surface

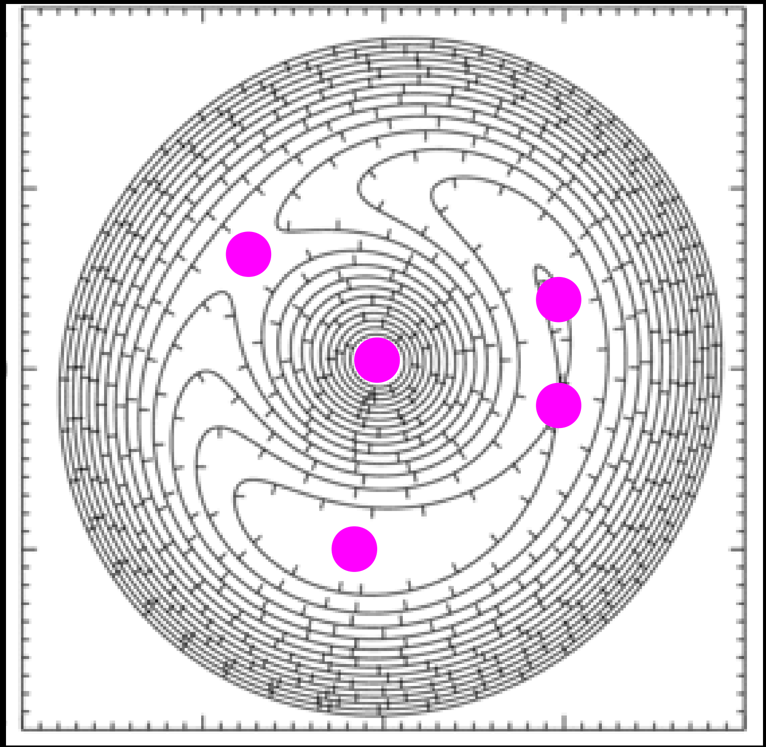

Fermat's principle: Light follows the path of least time

Combine a **geometrical delay** with a **gravitational delay**

Images form at **stationary points** in surface

Weak lensing

A statistical measurement of **cosmic shear**

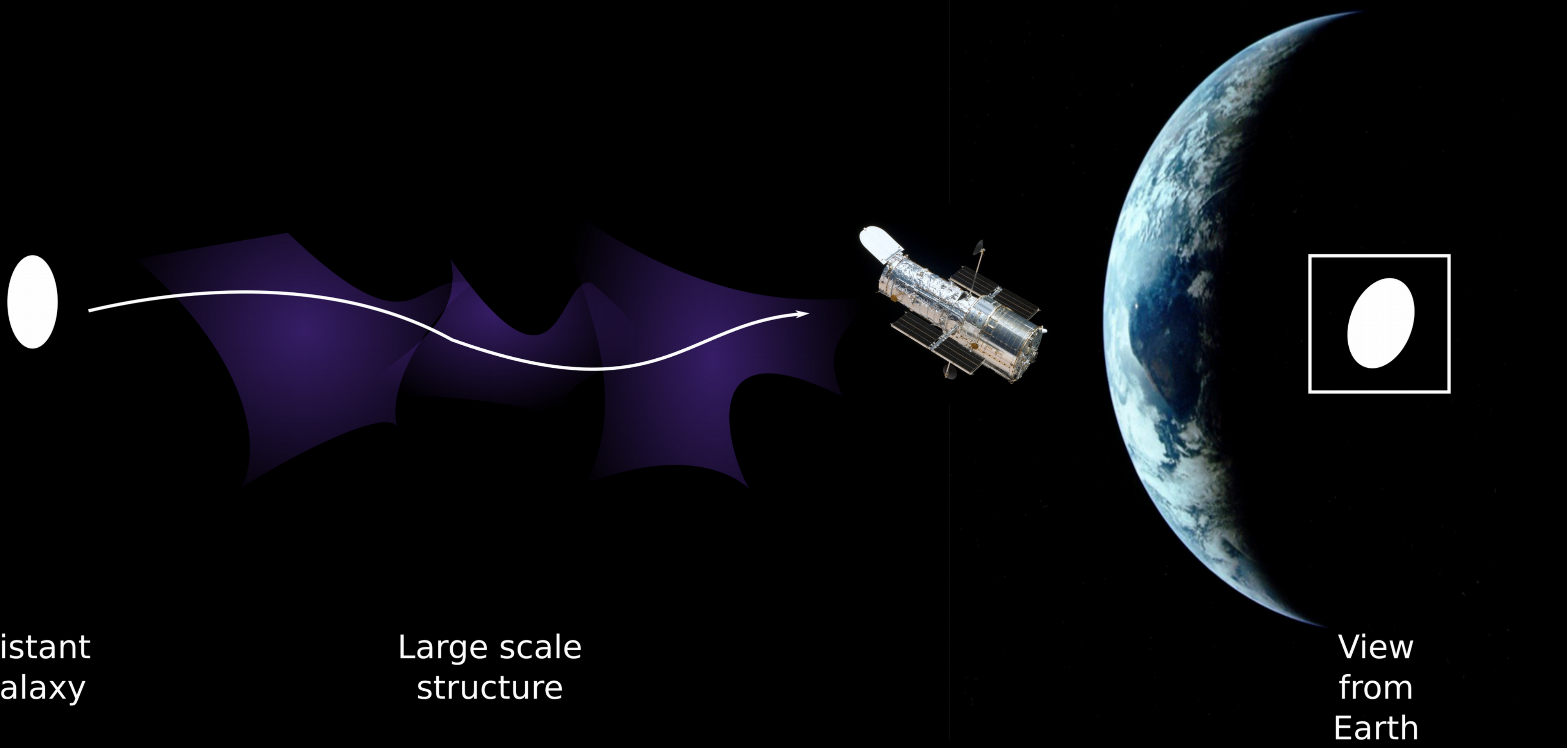

The University of Manchester

Weak lensing

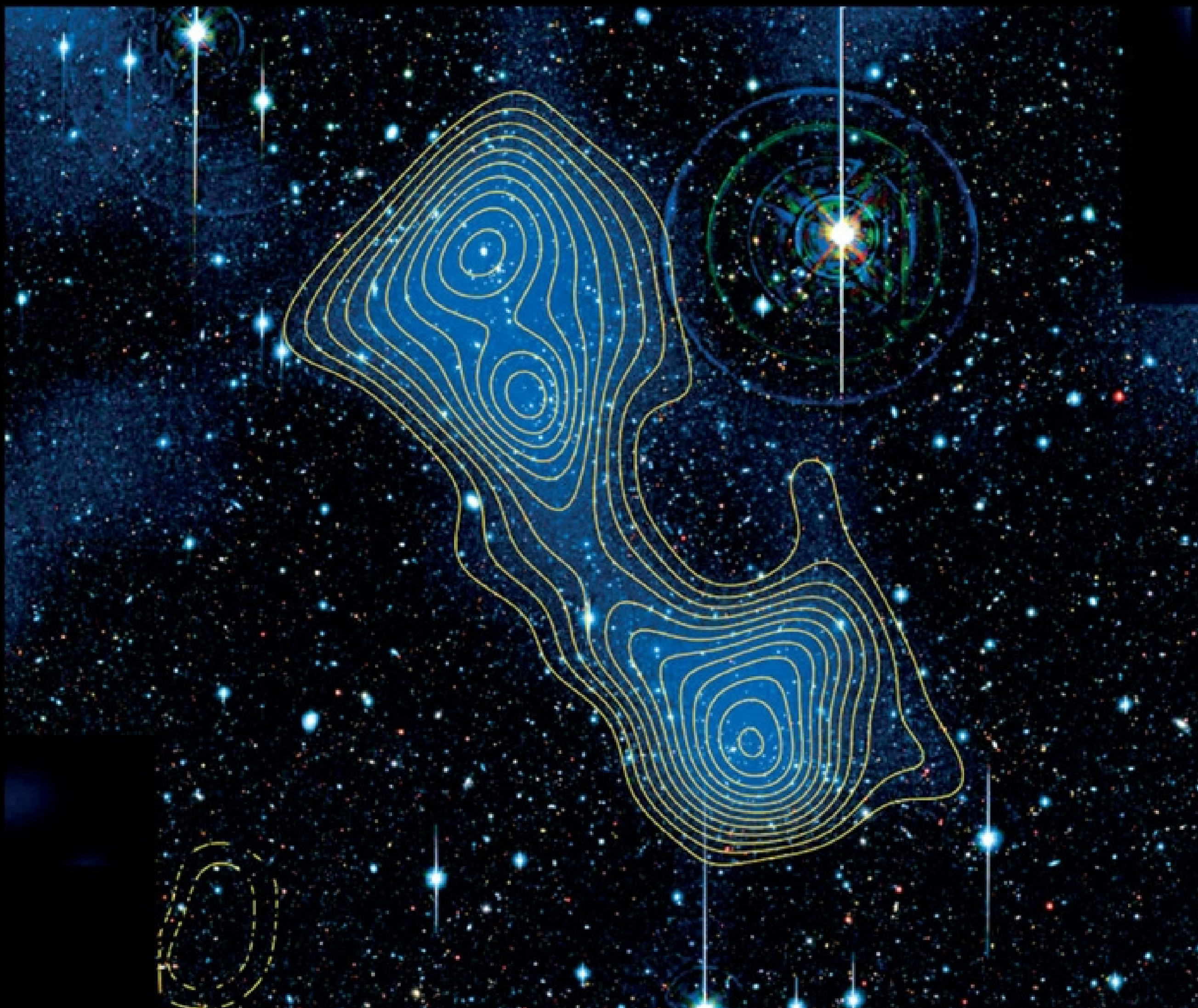

Image credit: J P Dietrich et al. 2012, Nature

8.2 m Subaru telescope on Mauna Kea, Hawaii

Two galaxy clusters 60 million light years apart

Shapes of more than 40 000 background galaxies measured

Mass reconstructed to find a dark matter filament connecting the clusters

Microlensing

Compact projected mass exceeds **critical density**

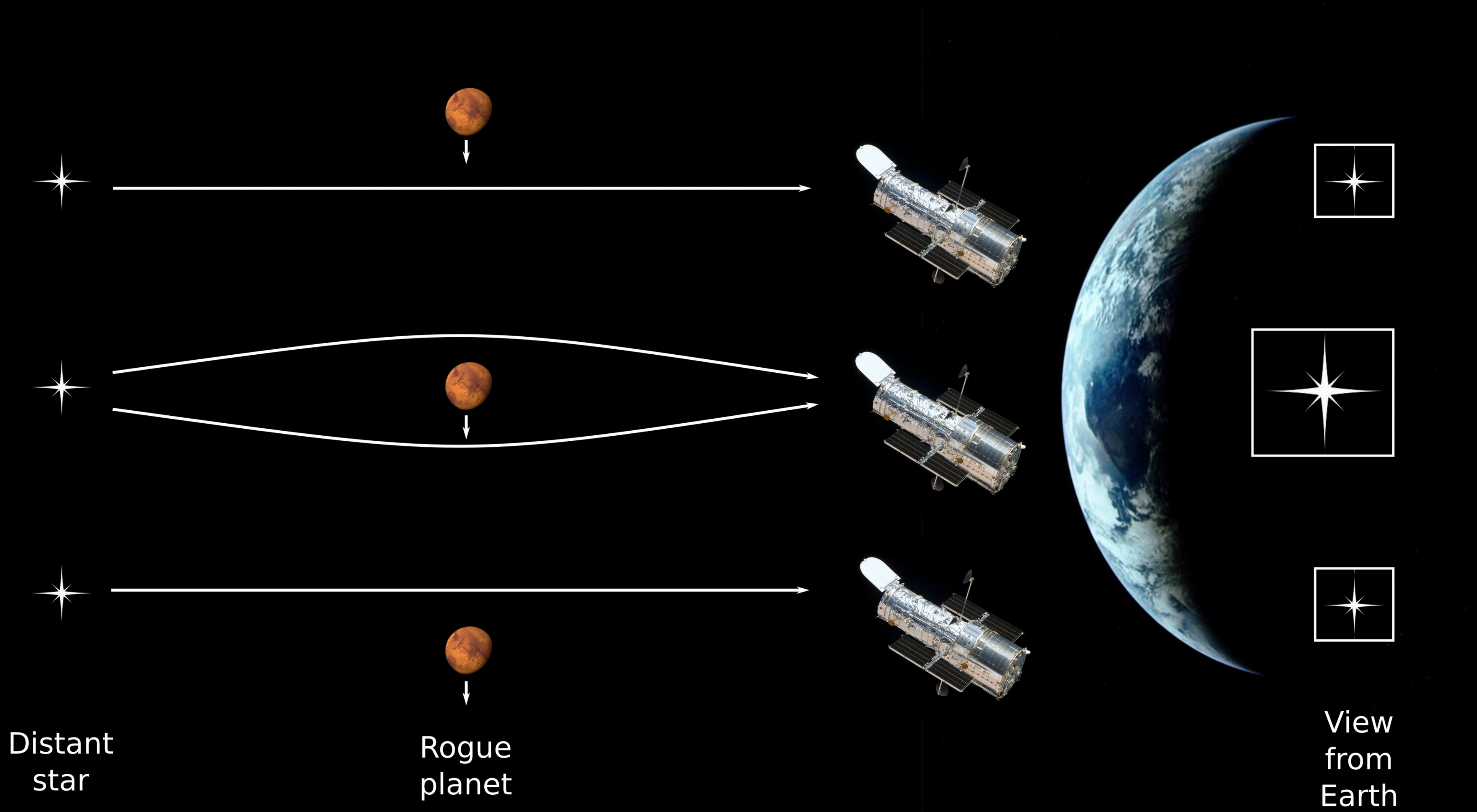

Microlensing

The brightening of a background star due to the lensing effect of an invisible red dwarf

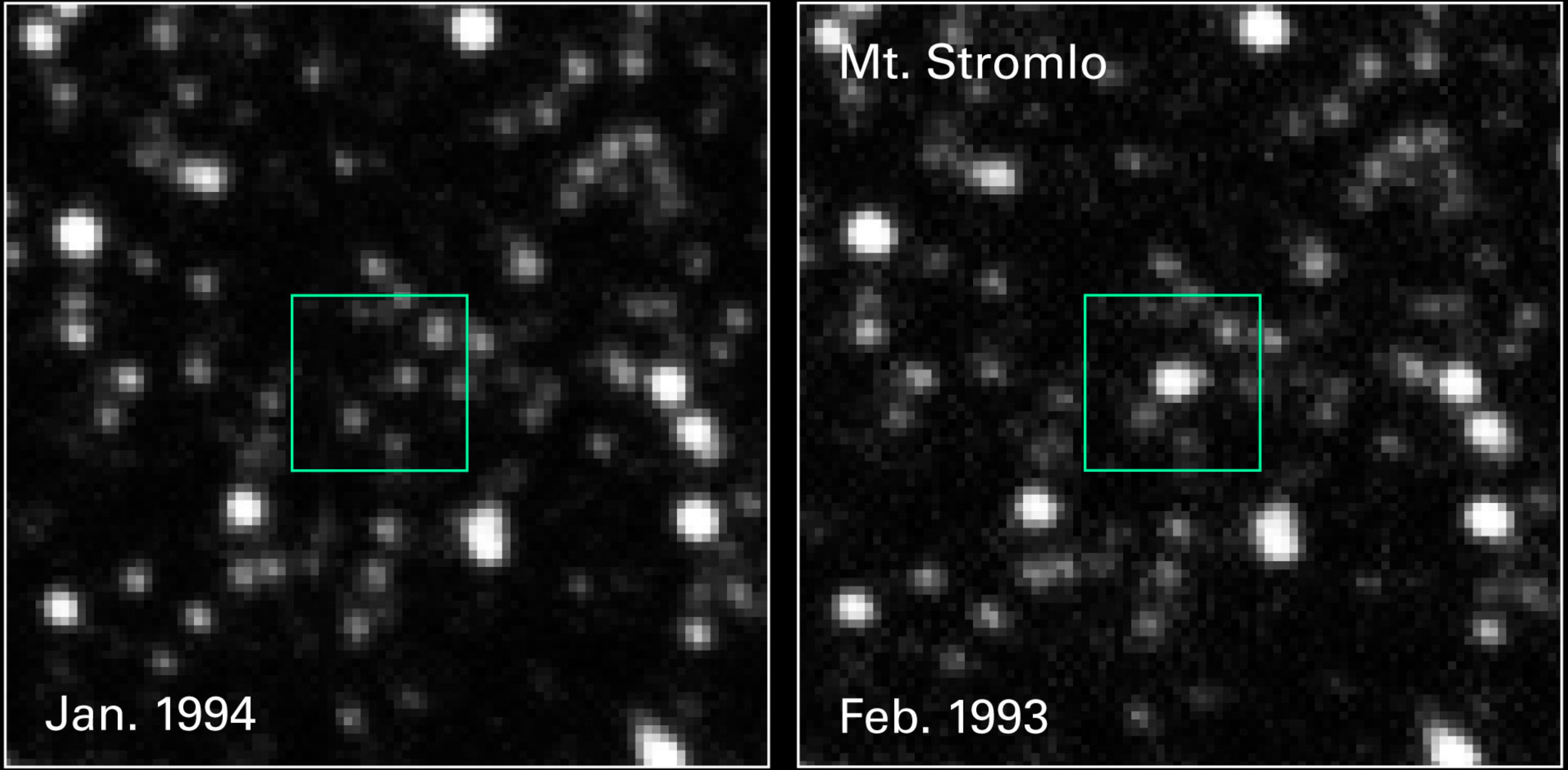

Credit: NASA/ESA Hubble, D. Bennett

Strong lensing

Extended projected lens mass exceeds **critical density**

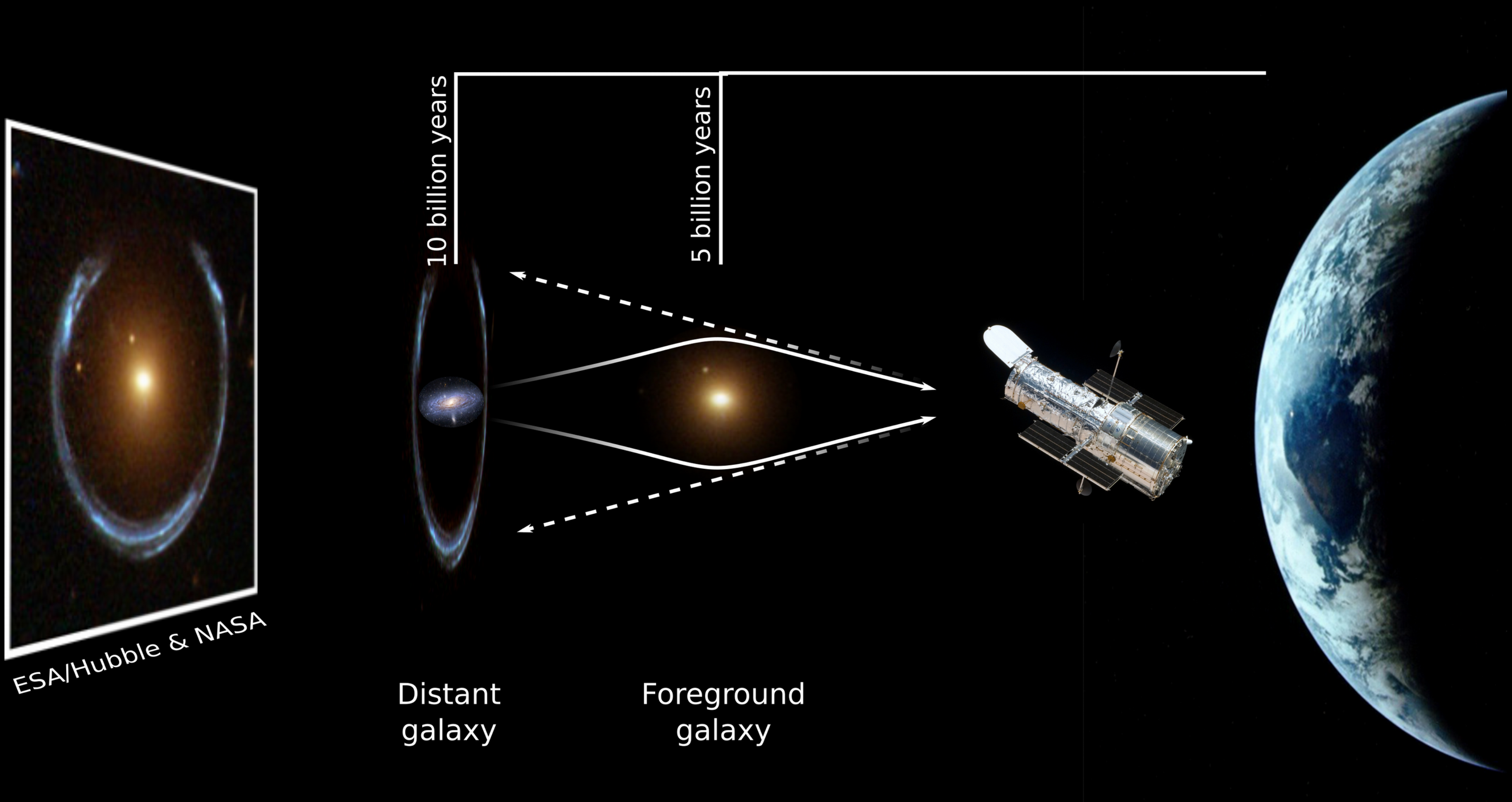

Strong lensing configurations

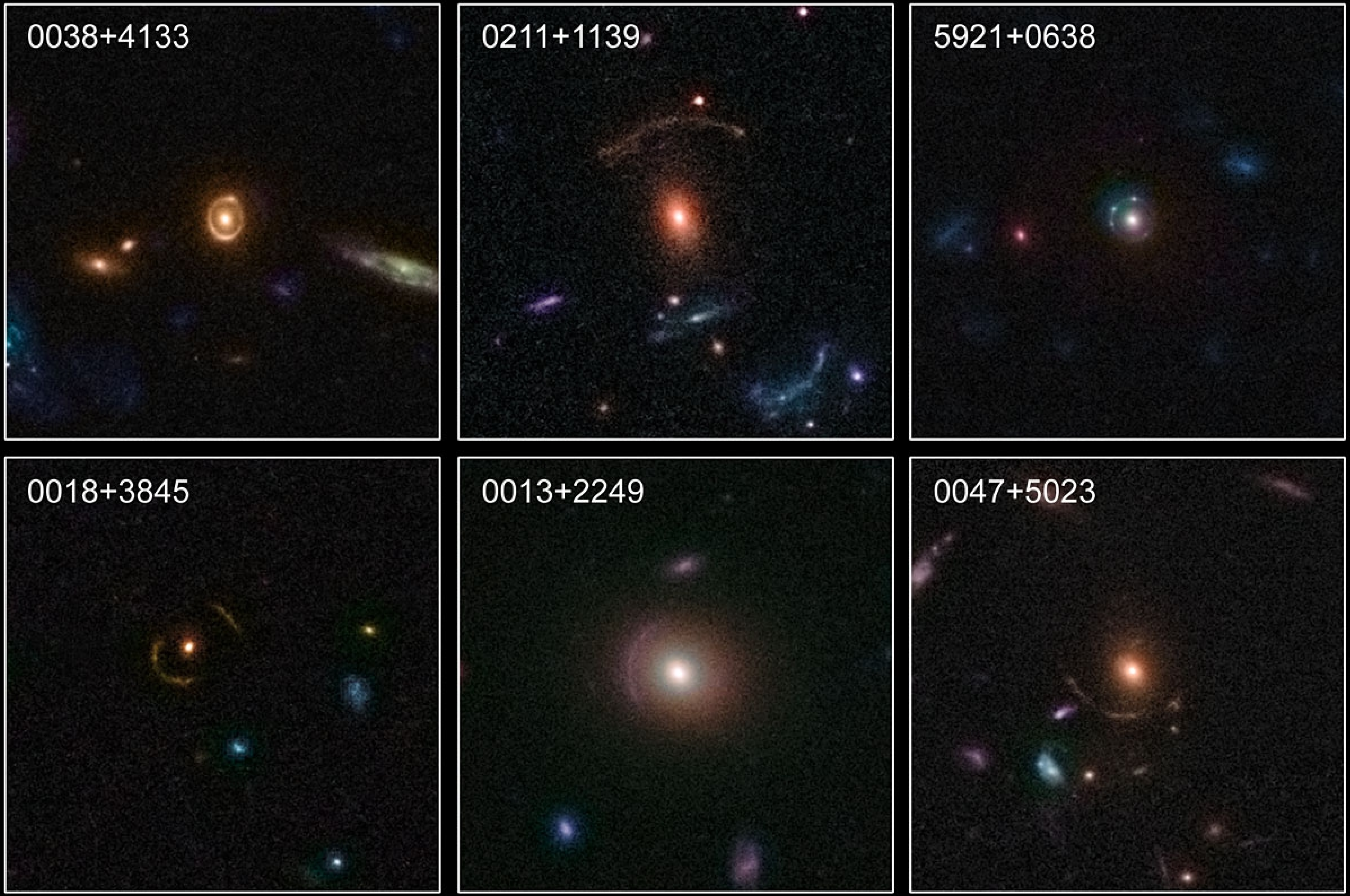

Credit: NASA/ESA Hubble

Science from lenses: dark matter structure

- Sub-galactic structure gives rise to image anomalies

Millenium simulation of dark matter haloes

Moore at al. 1999

Dark matter power spectrum

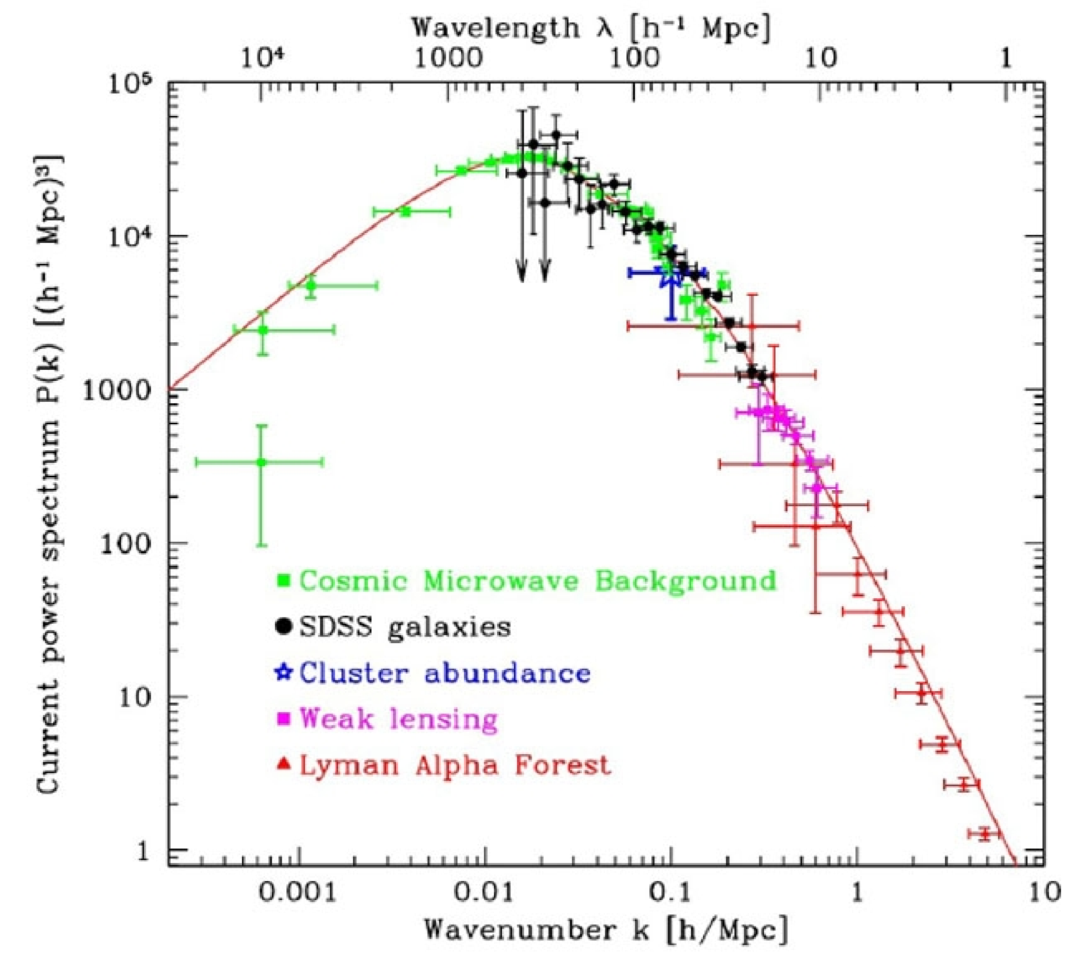

Science from lenses: the Hubble parameter

Measure **time delay** between images

Measure and model lensing galaxy

Infer time delay distance

Convert into cosmological parameters

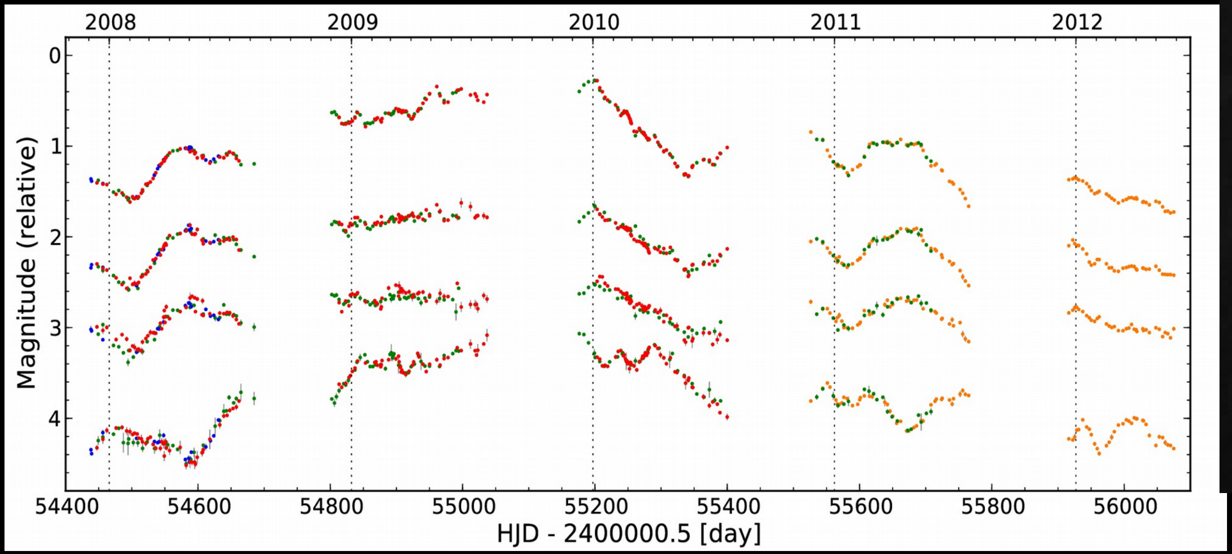

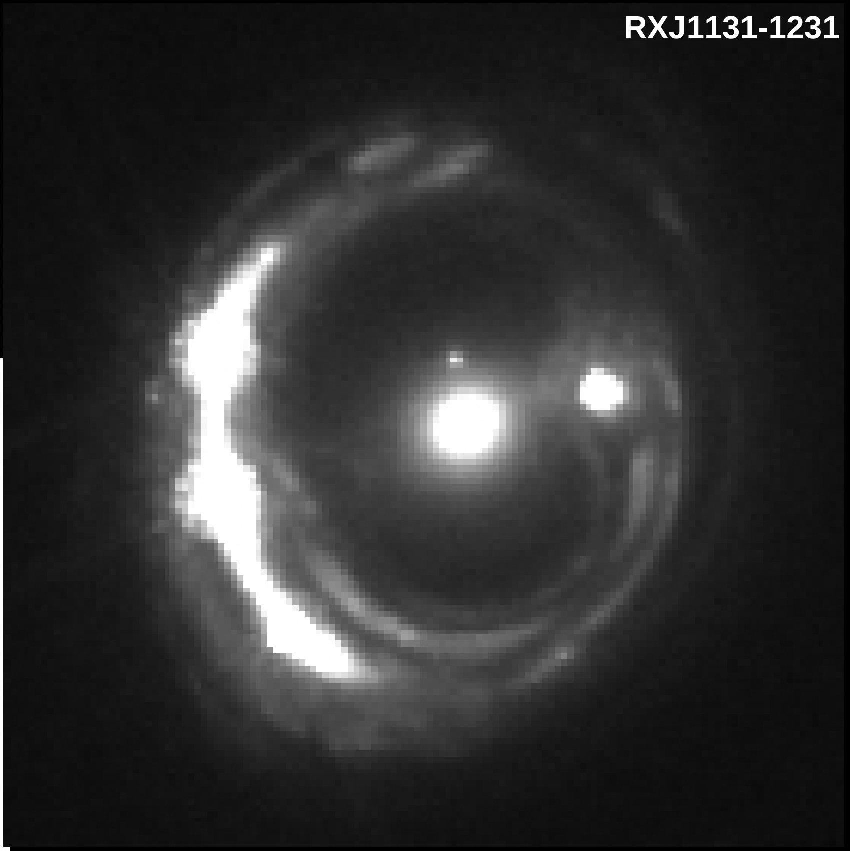

Suyu, Treu et al. 2014

Science from lenses: cosmic telescopes

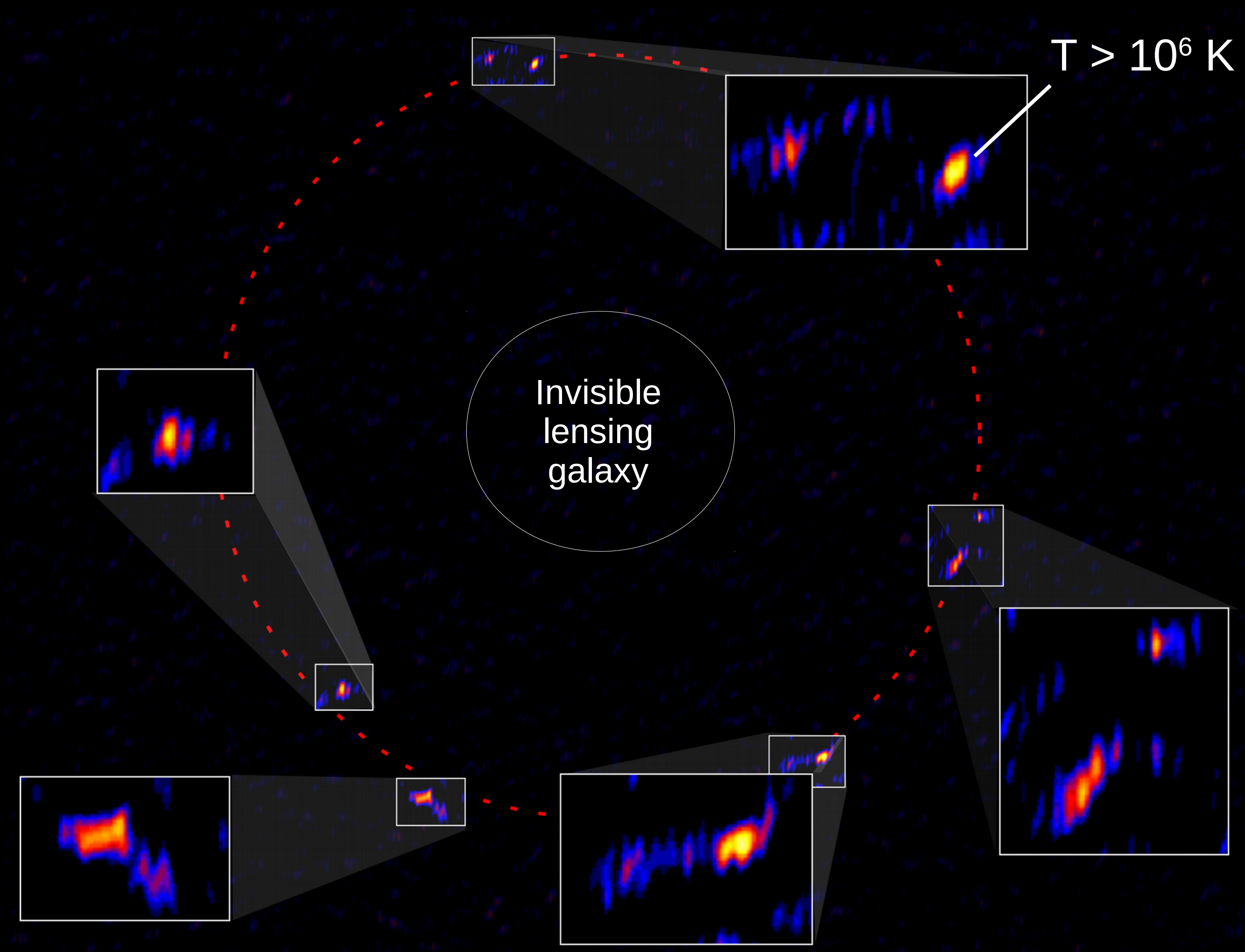

A quasar jet is lensed into four separate images

The lensing galaxy is invisible at radio wavelength

Lensing results in x50 magnification of this quasar

We can measure the temperature and morphology of this otherwise unseen object

Hartley et al., in prep. 2017

Science from lenses: cosmic telescopes

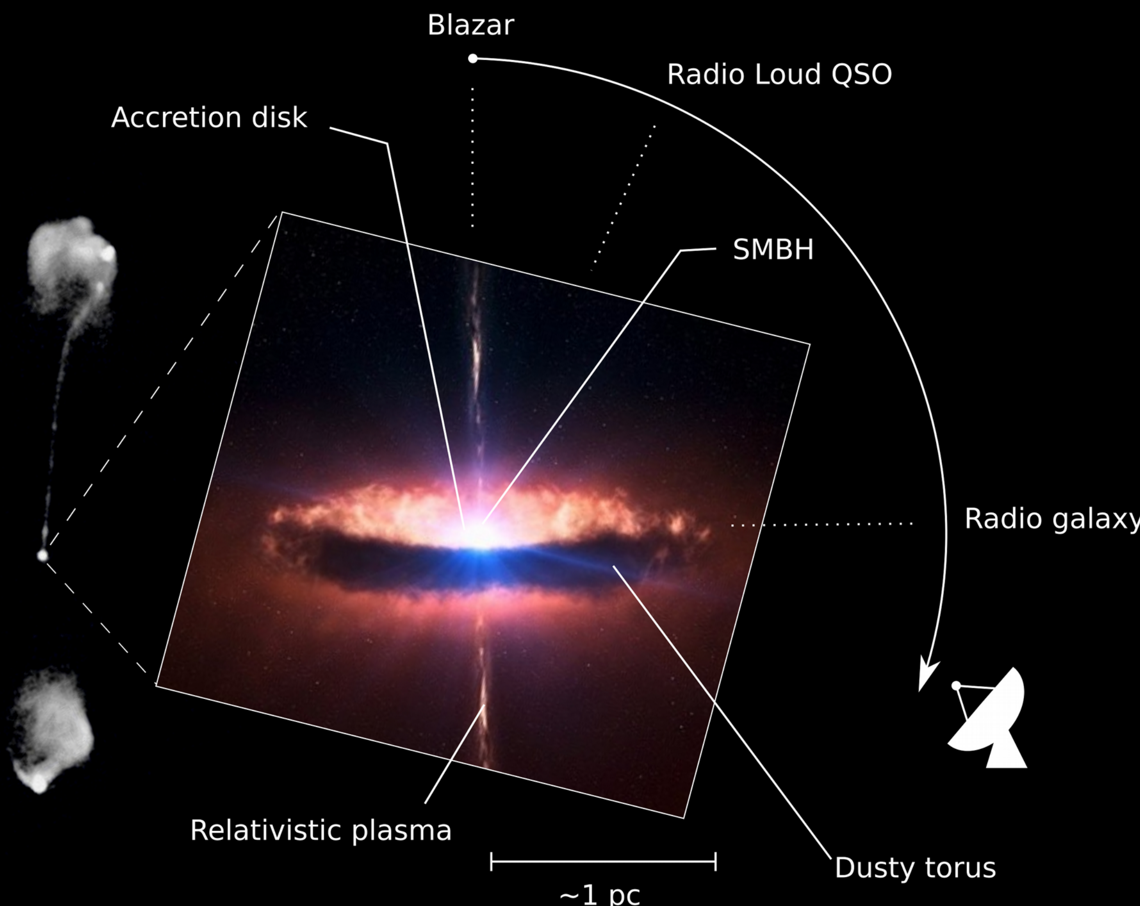

Active galactic nucleus (AGN)

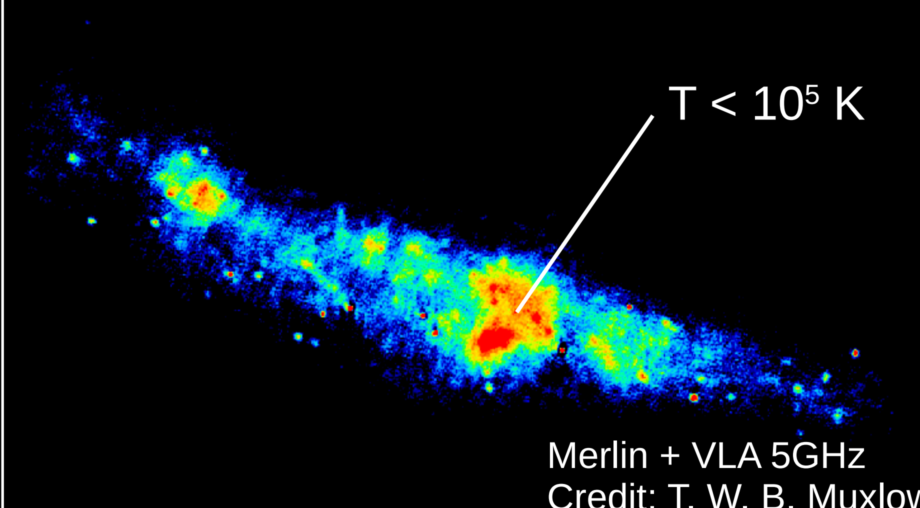

Starburst regions

Science from lenses: with a larger sample

Lensing allows us to study galaxy evolution by looking at mass structure over cosmic time

N = 100 lenses

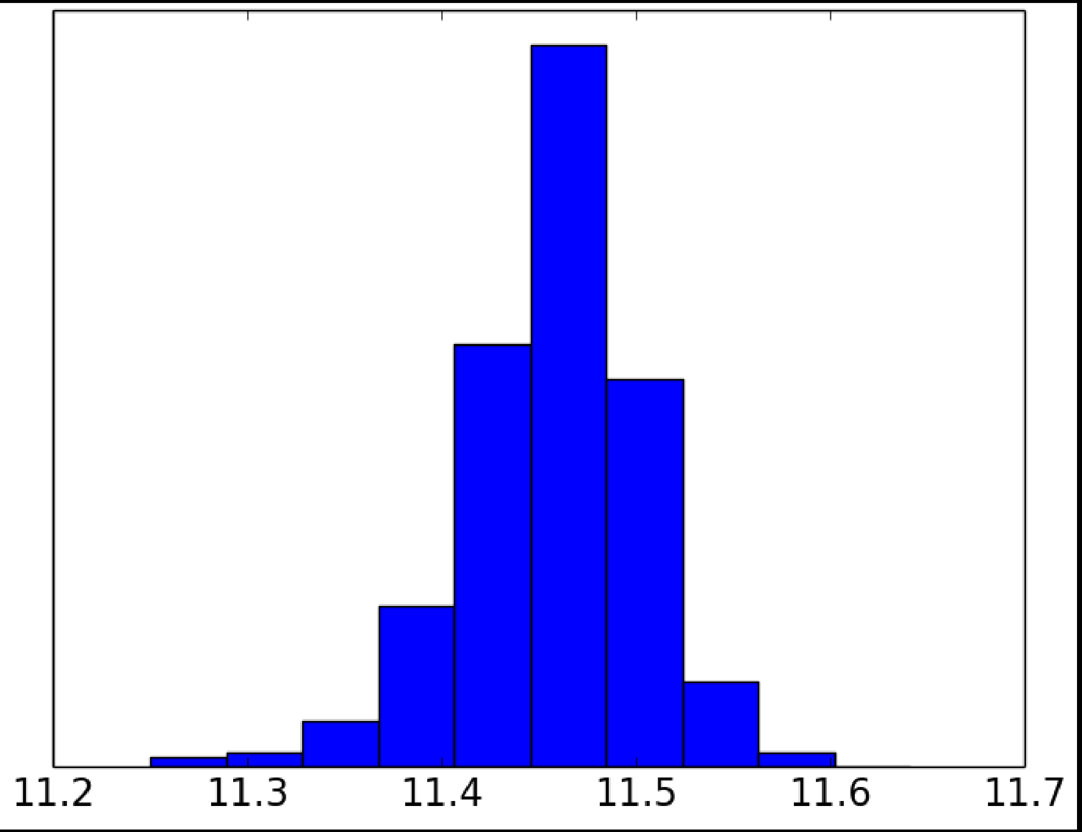

stellar mass

A. Tagore et al. 2017

Science from lenses: with a larger sample

Lensing allows us to study galaxy evolution by looking at mass structure over cosmic time

N = 1 000 lenses

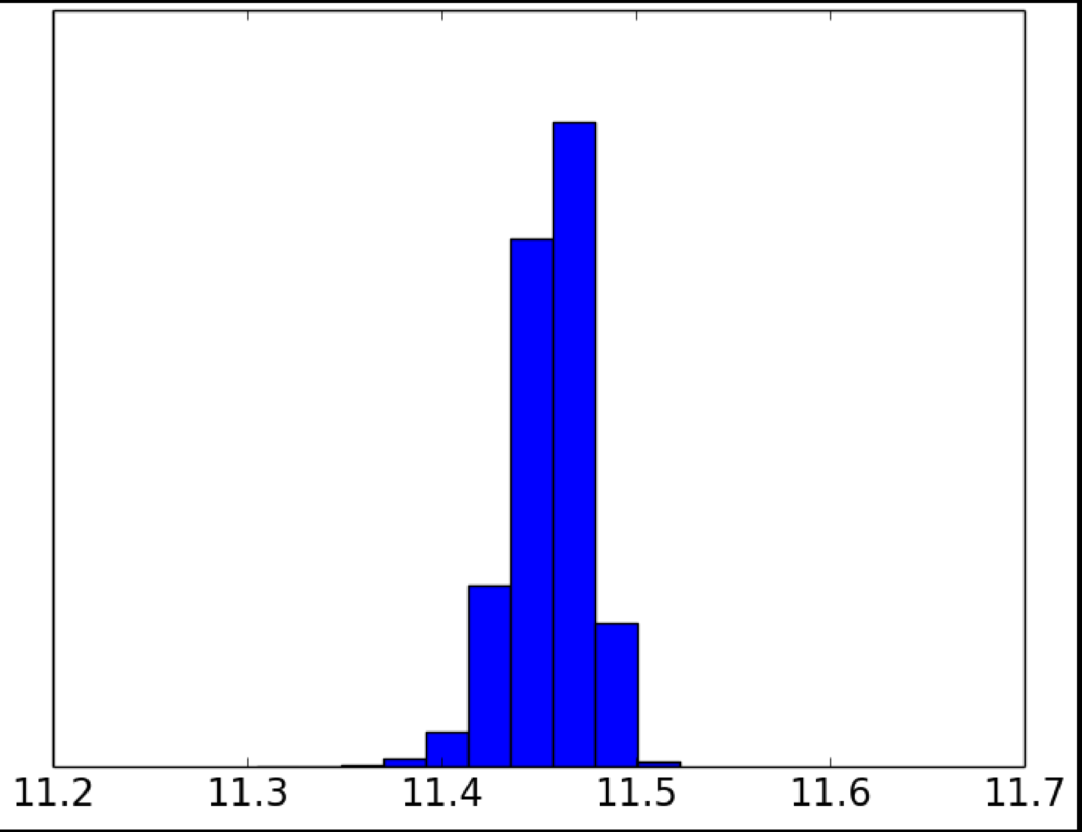

stellar mass

A. Tagore et al. 2017

Science from lenses: with a larger sample

Lensing allows us to study galaxy evolution by looking at mass structure over cosmic time

N = 100 000 lenses

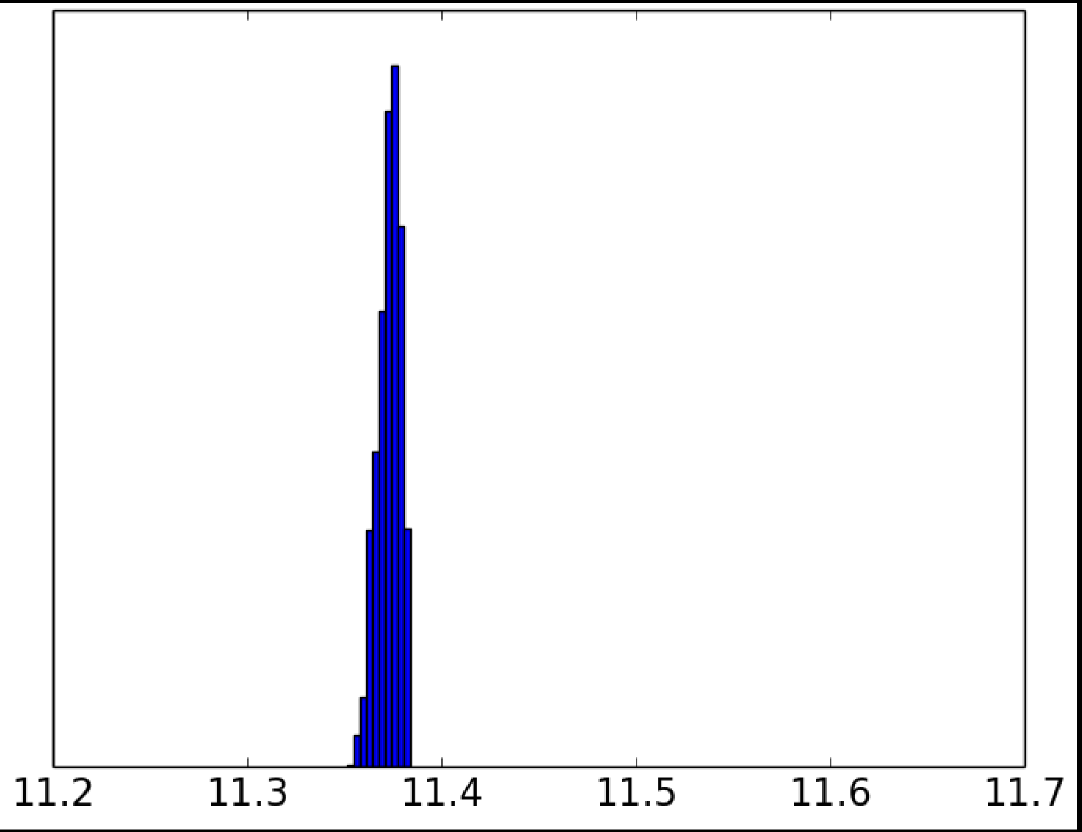

stellar mass

A. Tagore et al. 2017

The University of Manchester

Science from lenses: with a larger sample

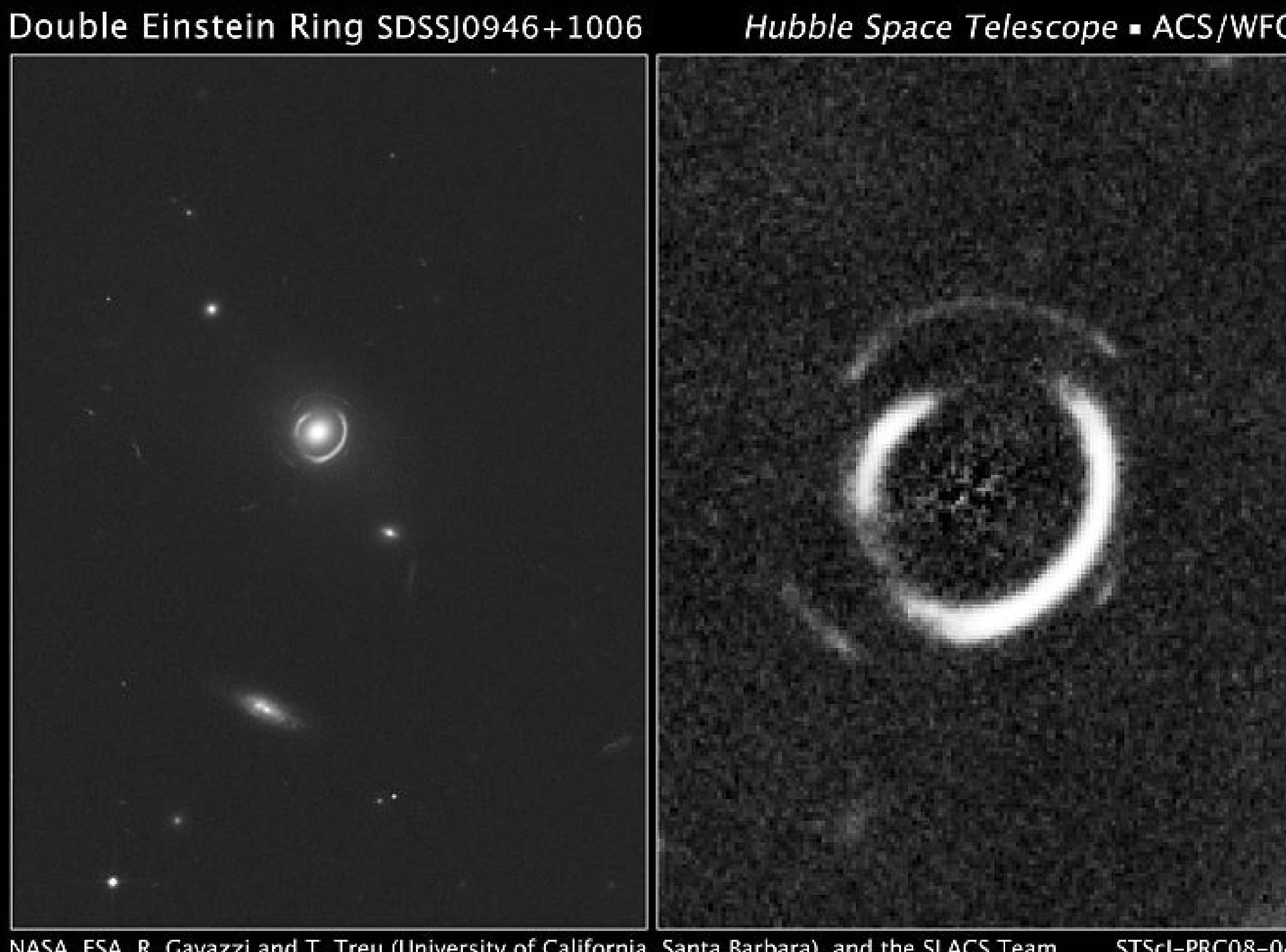

Double source plane lenses

MANCHESTER 1824
The University of Manchester

esa
LSST Large Synoptic Survey Telescope
ISSI INTERNATIONAL SPACE SCIENCE INSTITUTE

Euclid mission: Strong Lens Legacy Science Group

- *white paper in prep*.

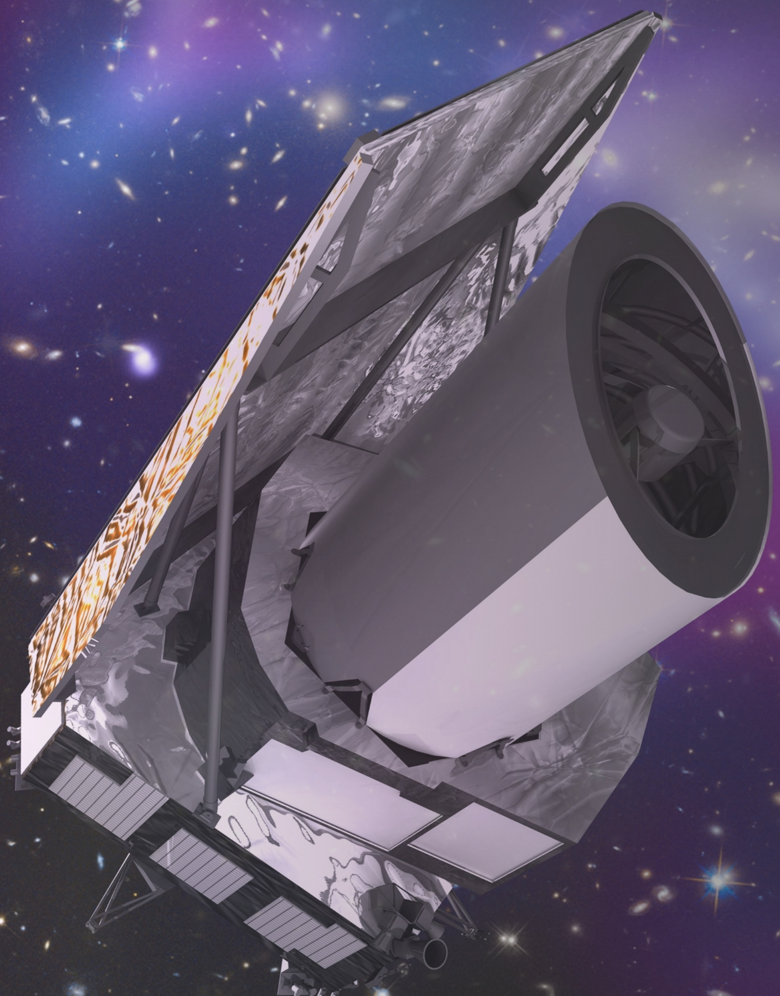

Current sample

~300 strong lenses

Expectations

~10 000 000 000 sources

~300 000 galaxy-galaxy lenses

~3000 cluster lenses

Where are they?

Support vector machines

$$\{\mathbf{x}_i, y_i\}, \quad i = 1, \cdots, l, \quad y_i \in \{-1, 1\}, \quad \mathbf{x}_i \in \mathbf{R}^d$$

$$\mathbf{x}_i \cdot \mathbf{w} + b \geq +1 \quad \text{for } y_i = +1$$
$$\mathbf{x}_i \cdot \mathbf{w} + b \leq -1 \quad \text{for } y_i = -1$$

$$L_P \equiv \frac{1}{2}\|\mathbf{w}\|^2 - \sum_{i=1}^{l} \alpha_i y_i (\mathbf{x}_i \cdot \mathbf{w} + b) + \sum_{i=1}^{l} \alpha_i$$

$$\mathbf{w} = \sum_i \alpha_i y_i \mathbf{x}_i \qquad \sum_i \alpha_i y_i = 0.$$

$$L_D = \sum_i \alpha_i - \frac{1}{2} \sum_{i,j} \alpha_i \alpha_j y_i y_j \mathbf{x}_i \cdot \mathbf{x}_j$$

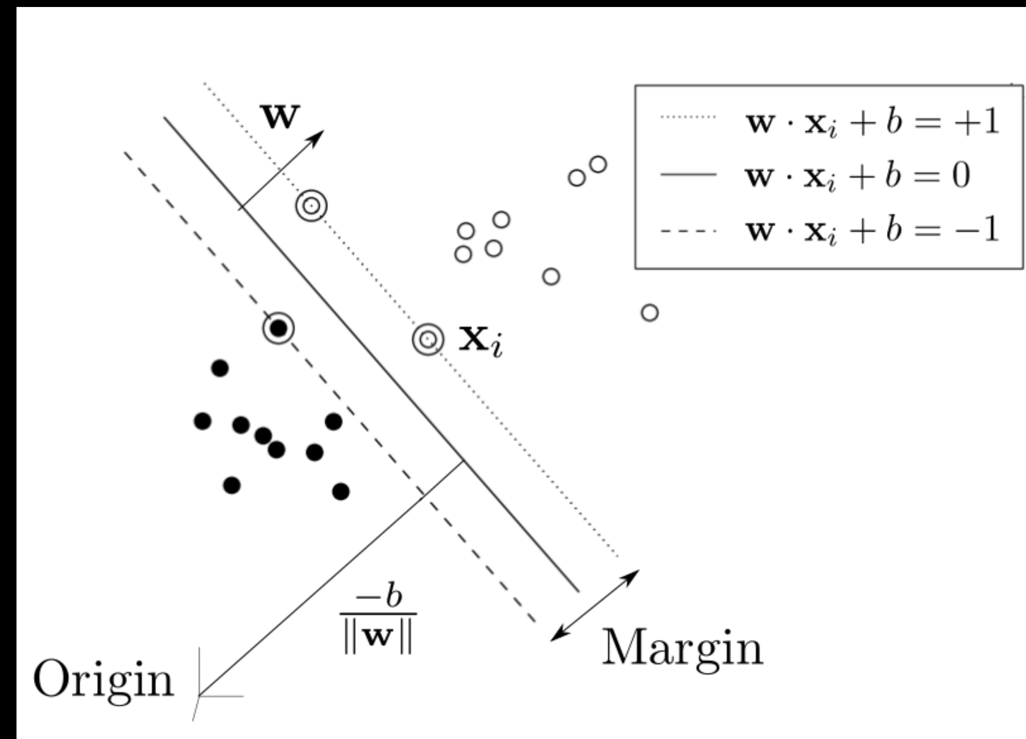

Vapnik et al. 1979, Cortes & Vapnik 1995

- Find optimal hyperplane separating two classes of data
- Optimisation depends only on dot products of support vectors, found on the edge of each class

MANCHESTER 1824
The University of Manchester

esa LSST Large Synoptic Survey Telescope ISSI International Space Science Institute

Support vector machines

$$\{\mathbf{x}_i, y_i\}, \quad i = 1, \cdots, l, \; y_i \in \{-1, 1\}, \; \mathbf{x}_i \in \mathbf{R}^d$$

$$\mathbf{x}_i \cdot \mathbf{w} + b \geq +1 \quad \text{for } y_i = +1$$
$$\mathbf{x}_i \cdot \mathbf{w} + b \leq -1 \quad \text{for } y_i = -1$$

$$L_P \equiv \frac{1}{2}\|\mathbf{w}\|^2 - \sum_{i=1}^{l} \alpha_i y_i (\mathbf{x}_i \cdot \mathbf{w} + b) + \sum_{i=1}^{l} \alpha_i$$

$$\mathbf{w} = \sum_i \alpha_i y_i \mathbf{x}_i \qquad \sum_i \alpha_i y_i = 0.$$

$$L_D = \sum_i \alpha_i - \frac{1}{2}\sum_{i,j} \alpha_i \alpha_j y_i y_j \mathbf{x}_i \cdot \mathbf{x}_j$$

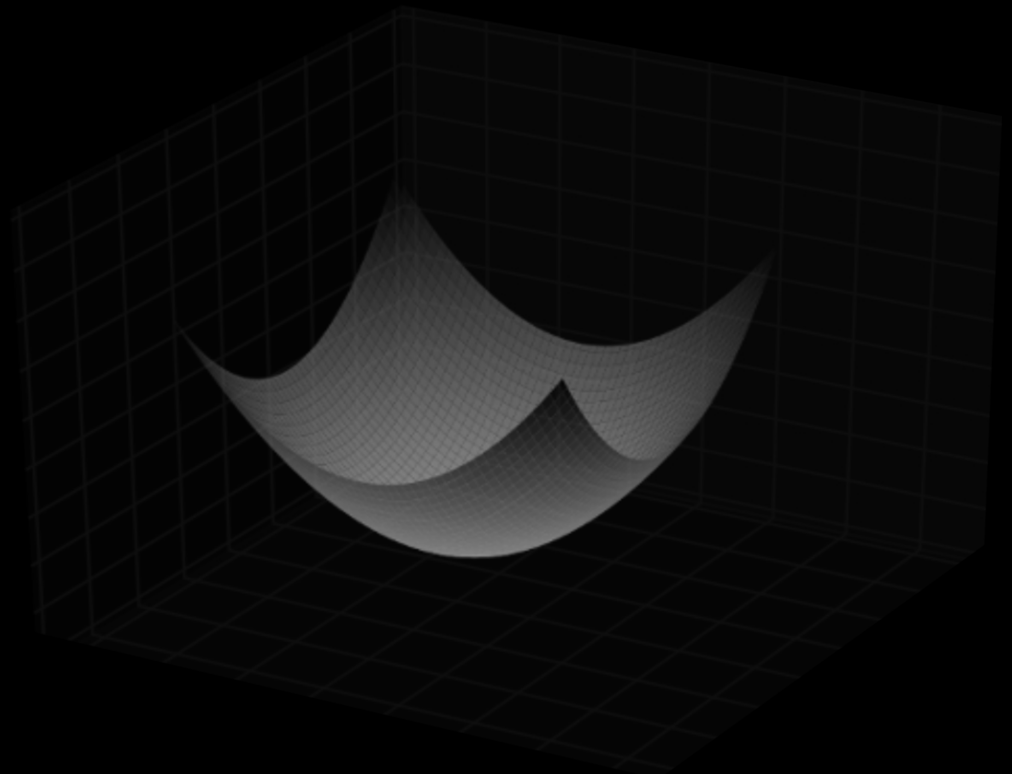

Vapnik et al. 1979, Cortes & Vapnik 1995

- Function is convex: every local solution is a global one – no local minima

MANCHESTER 1824
The University of Manchester

esa
Large Synoptic Survey Telescope
INTERNATIONAL SPACE SCIENCE INSTITUTE

Support vector machines

$$\{\mathbf{x}_i, y_i\}, \quad i = 1, \cdots, l, \quad y_i \in \{-1, 1\}, \quad \mathbf{x}_i \in \mathbf{R}^d$$

$$\mathbf{x}_i \cdot \mathbf{w} + b \geq +1 \quad \text{for } y_i = +1$$
$$\mathbf{x}_i \cdot \mathbf{w} + b \leq -1 \quad \text{for } y_i = -1$$

$$K(\mathbf{x}_i, \mathbf{x}_j) = \phi(\mathbf{x}_i) \cdot \phi(\mathbf{x}_j).$$

$$\mathbf{w} = \sum_i \alpha_i y_i \mathbf{x}_i \qquad \sum_i \alpha_i y_i = 0.$$

$$L_D = \sum_i \alpha_i - \frac{1}{2} \sum_{i,j} \alpha_i \alpha_j y_i y_j \mathbf{x}_i \cdot \mathbf{x}_j$$

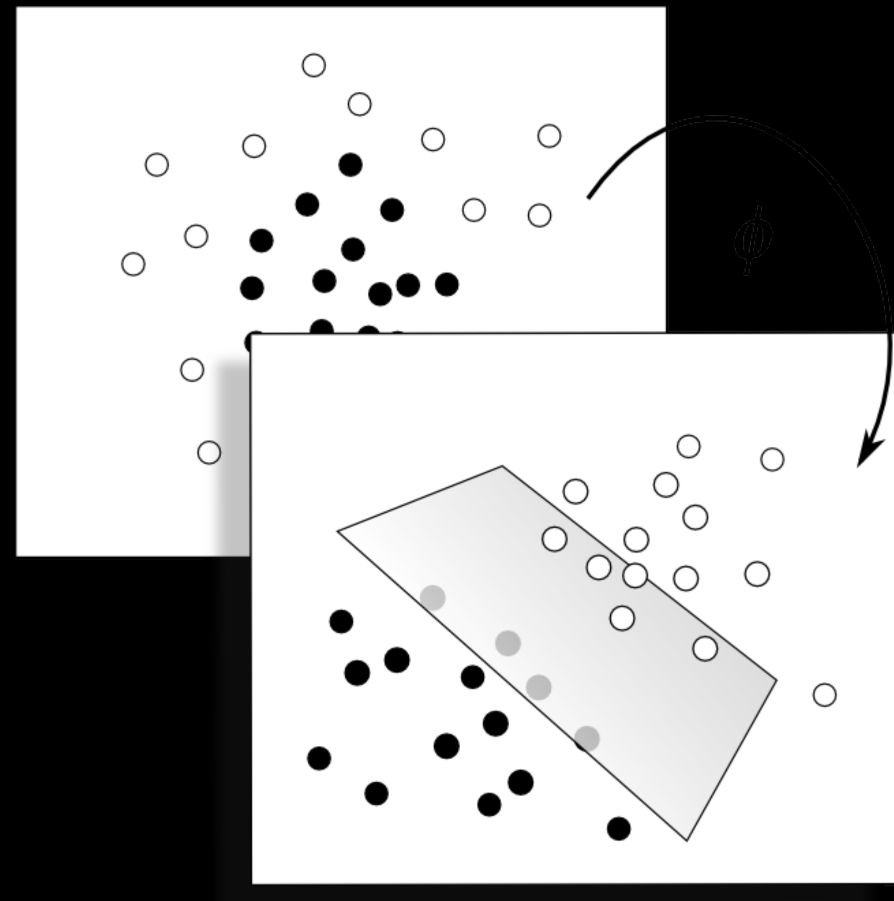

Boser et al. 1992

- Coordinate transformation can deal with non-linear separation
- Unknown kernel function replaces dot product

Feature extraction

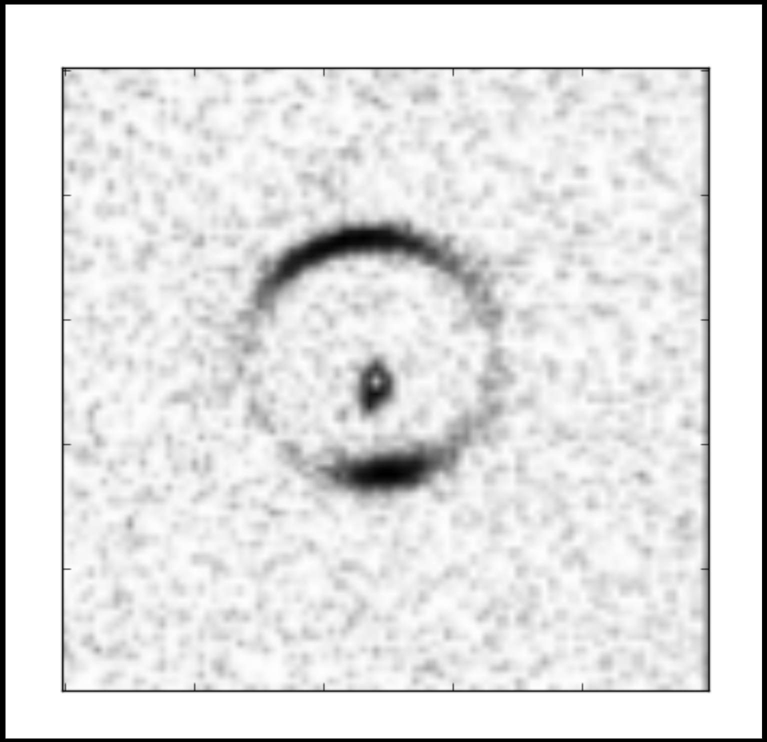

100 * 100 pixels = **10 000** features

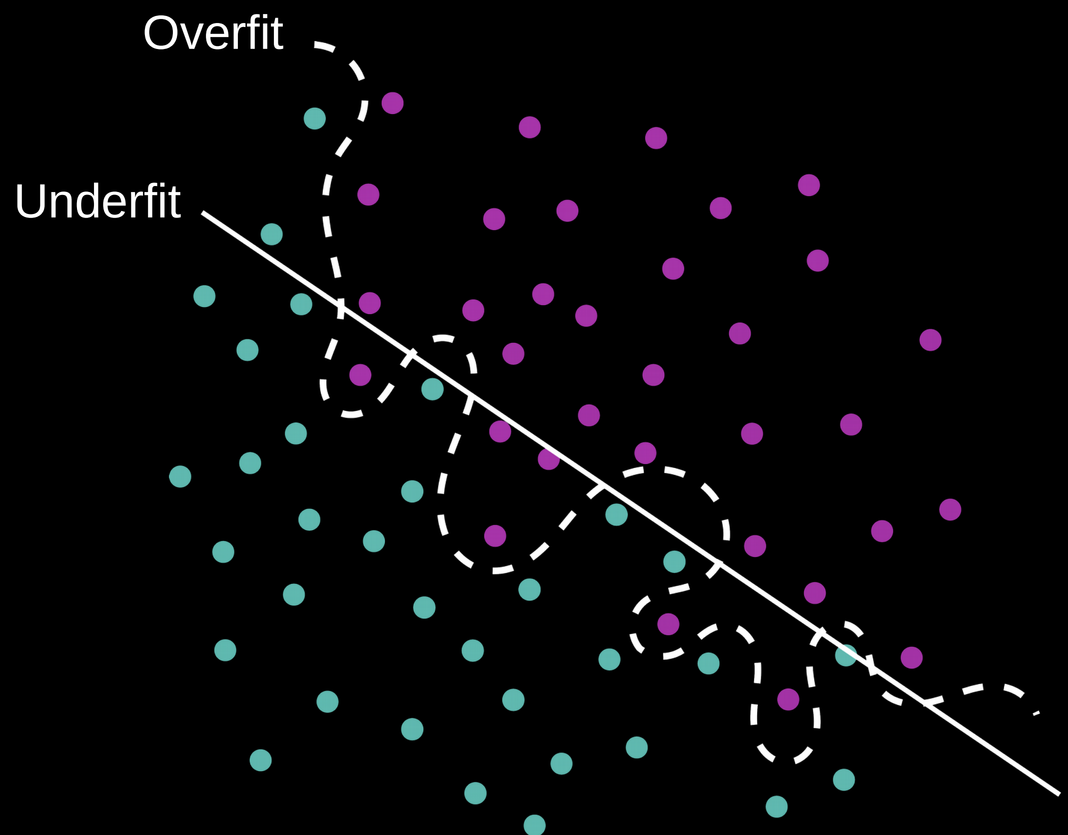

Feature extraction

Apply **Gabor filters**: model the simple cells of the mammillian visual cortex (Marcelja 1980)

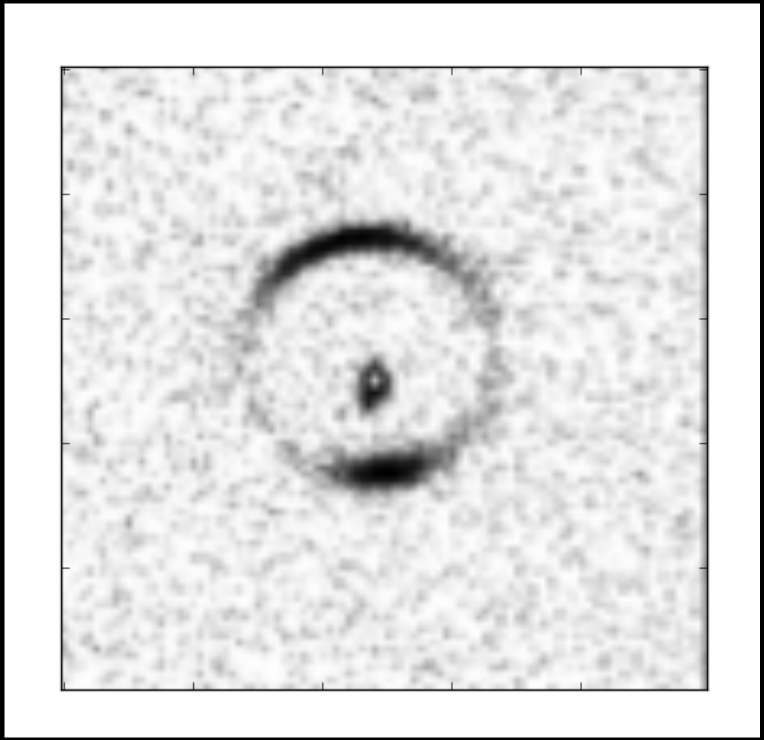

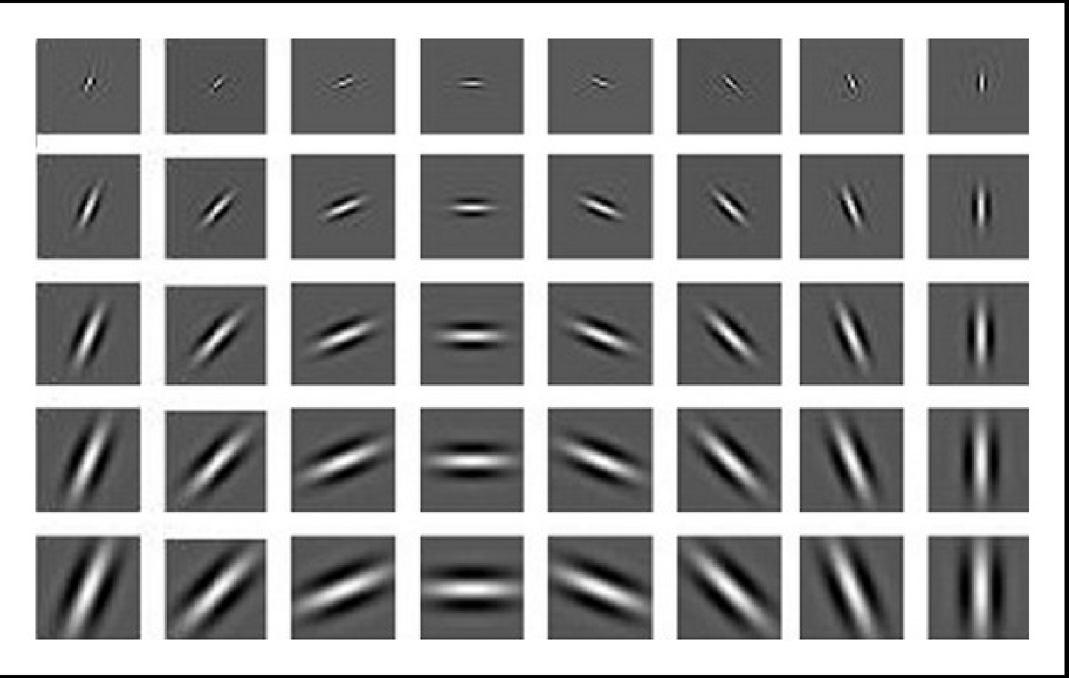

$$G_c[i,j] = Be^{-\frac{(i^2+j^2)}{2\sigma^2}} \cos\left(\frac{2\pi}{\lambda}(i\cos\theta + j\sin\theta)\right)$$

Feature extraction

Training sample ➡ polar transform ➡ Gabor filterbank ➡ calculate moments

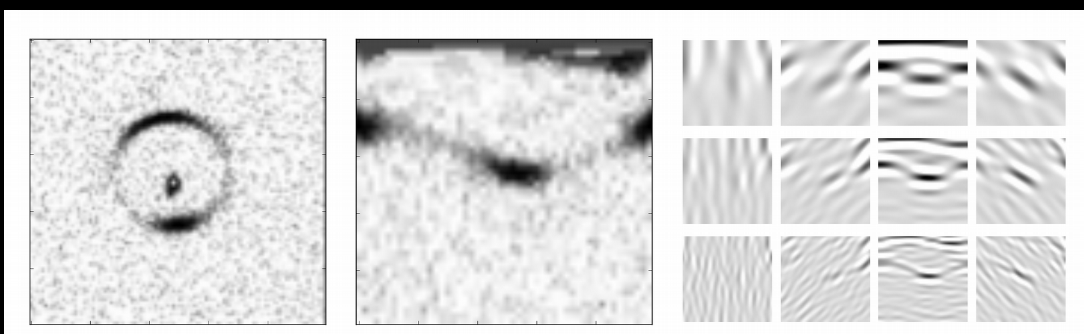

Mean	$\mu_1(x_1, \ldots, x_N) = \frac{1}{N} \sum_{j=1}^{N} x_j$
Variance	$\mu_2(x_1, \ldots, x_N) = \frac{1}{N-1} \sum_{j=1}^{N} (x_j - \mu_1)^2$
Skew	$\mu_3(x_1, \ldots, x_N) = \frac{1}{N} \sum_{j=1}^{N} \left[\frac{x_j - \mu_1}{\mu_2}\right]^3$
Kurtosis	$\mu_4(x_1, \ldots, x_N) = \left\{\frac{1}{N} \sum_{j=1}^{N} \left[\frac{x_j - \mu_1}{\mu_2}\right]^4\right\}$
Local energy	$E_s(x_1, \ldots, x_N) = \sum_{j=1}^{N} x_j^2$

Hartley et al. 2017 MNRAS

4 bands * 9 kernel frequencies * 7 kernel rotations * 5 moments = **1260** features

Feature selection

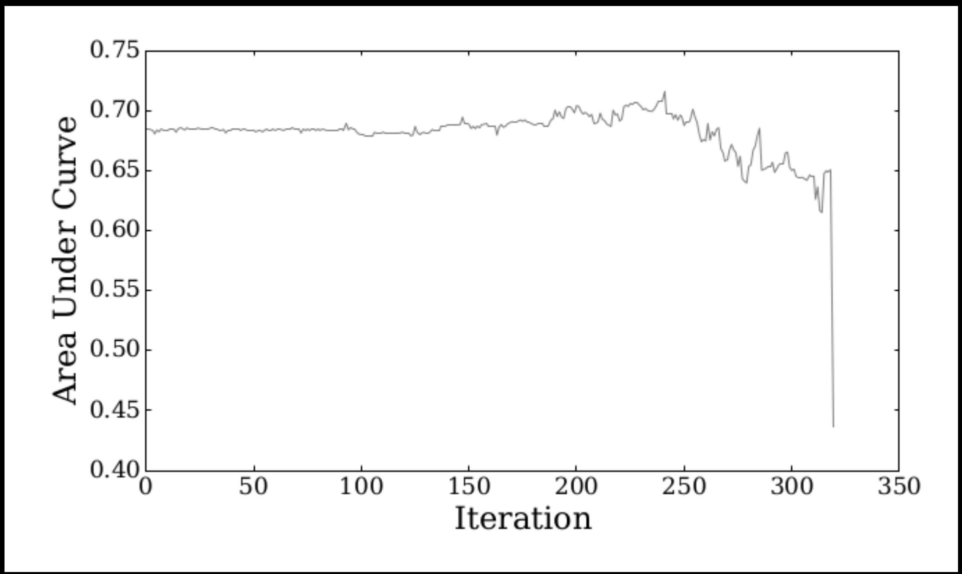

Recursive feature elimination

Simple, but can be unstable

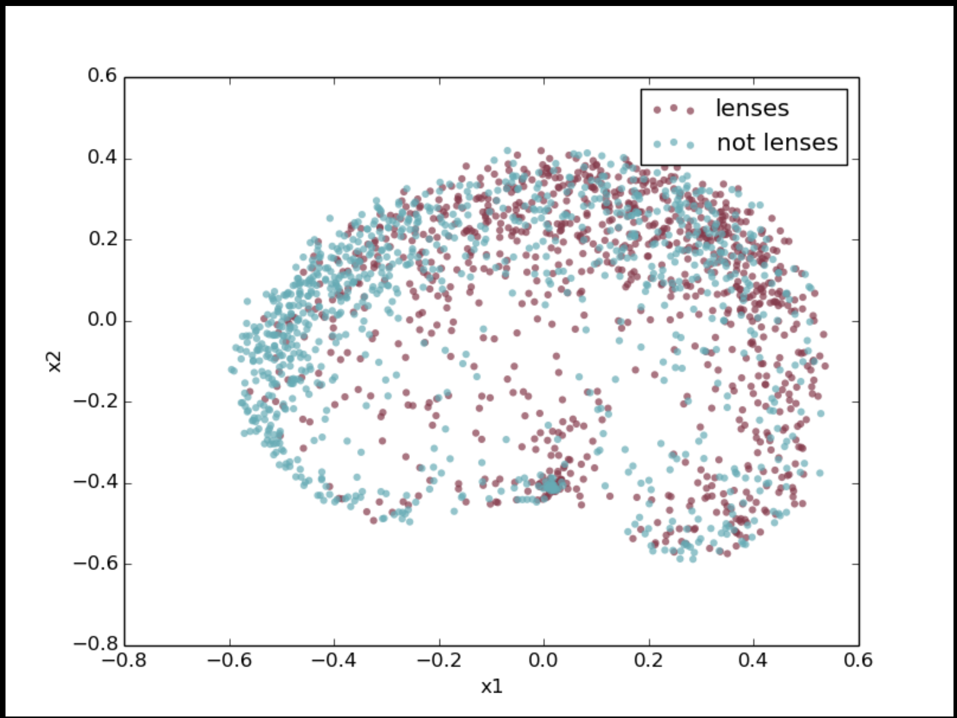

Principle component analysis

Feature selection

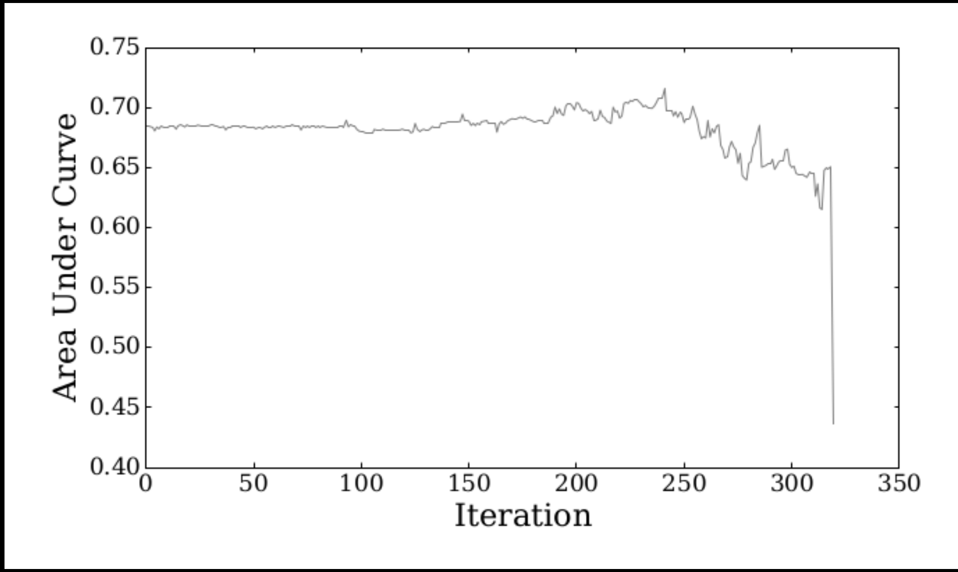

Recursive feature elimination

Simple, but can be unstable

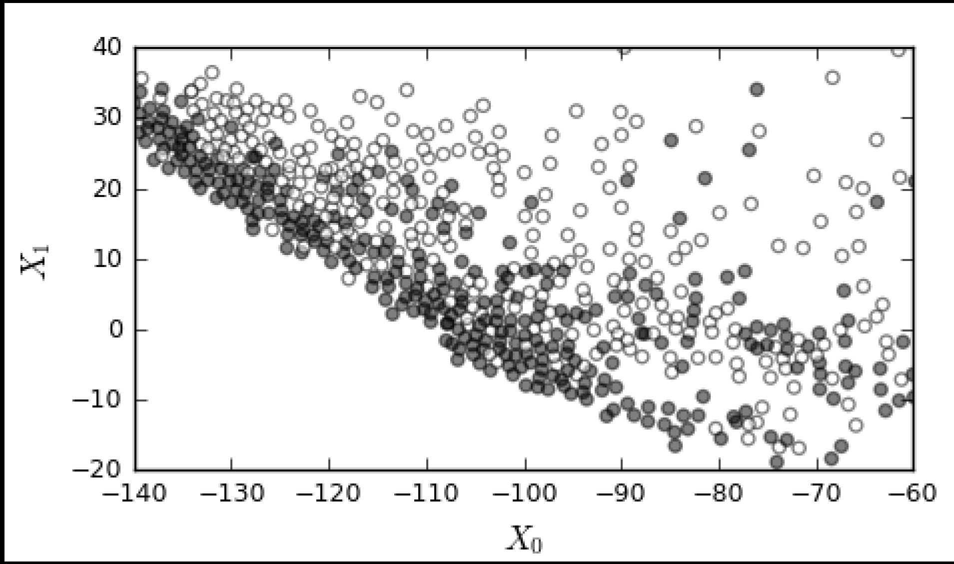

t-distributed stochastic neighbour embedding (t-SNE)

Like principle component analysis but able to respresent non-linear relationships

Feature selection

Stability selection:

Features are subsampled and perfomance evaluated

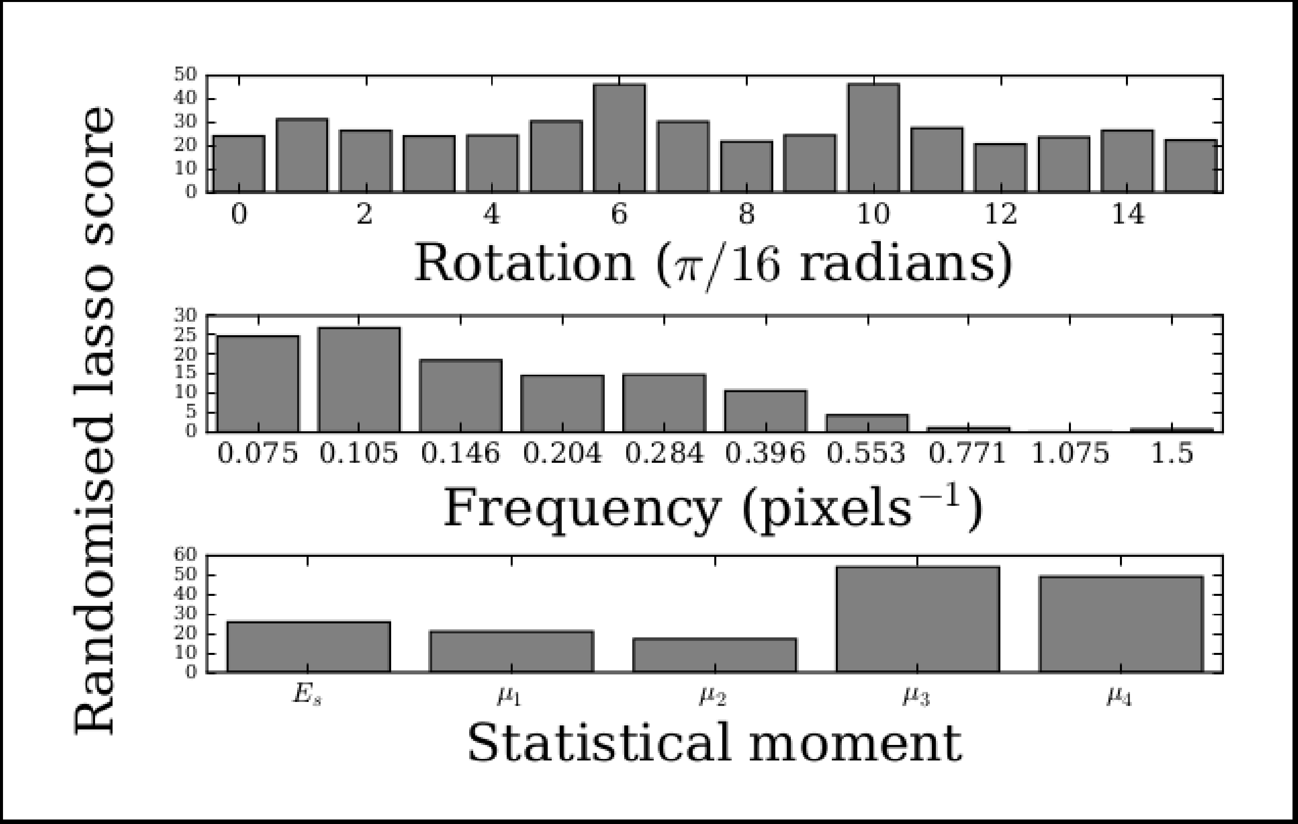

Model tuning

Regularisation parameters

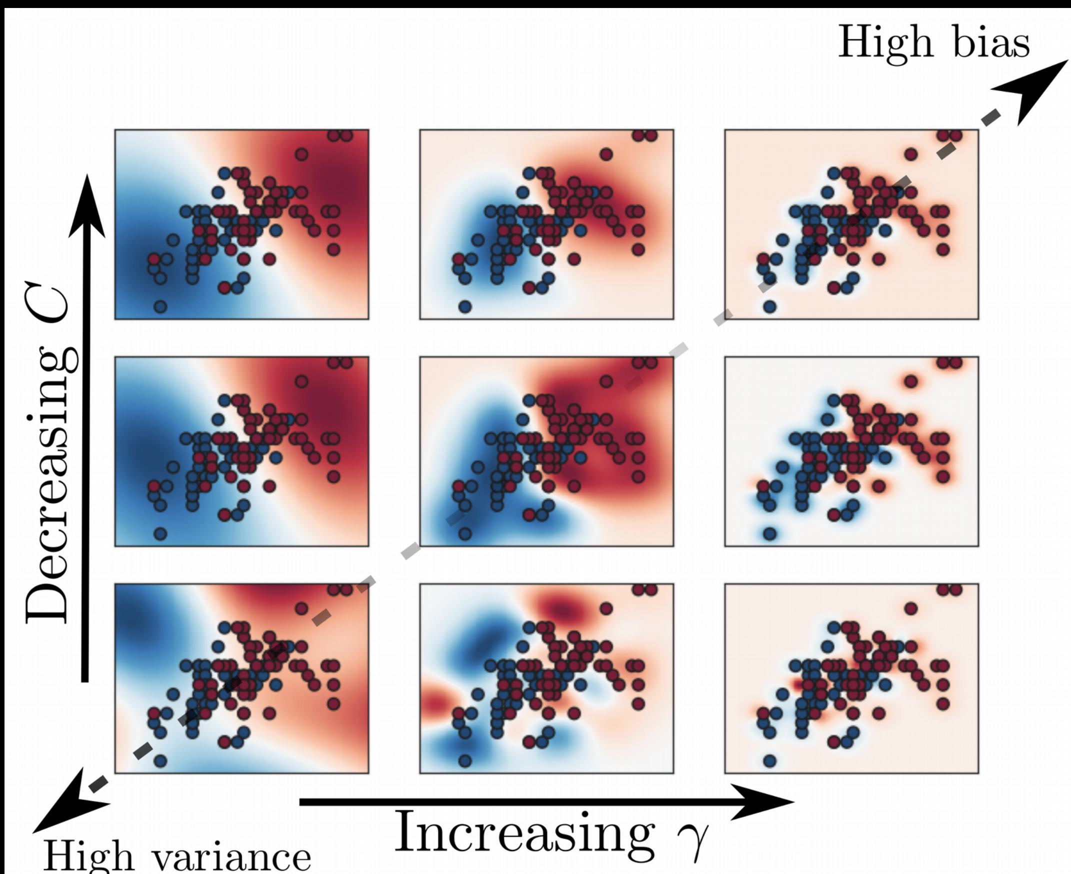

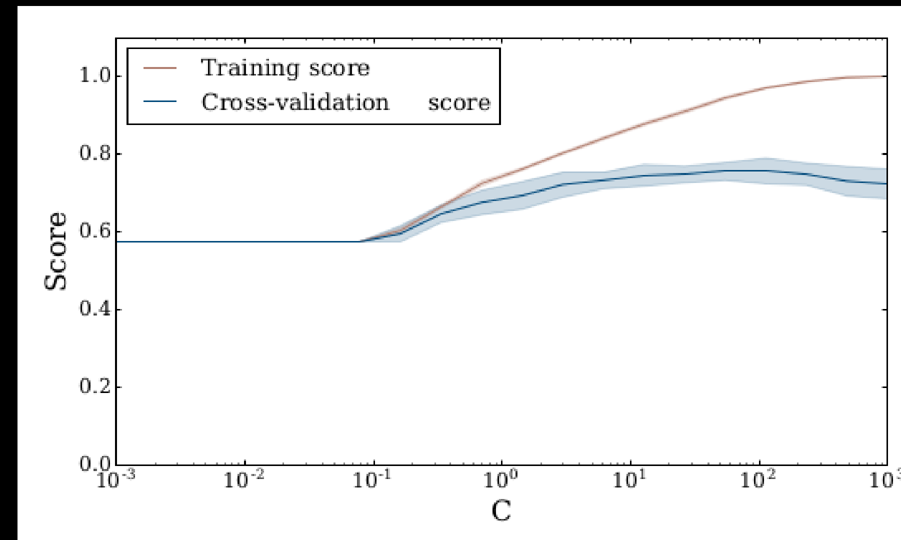

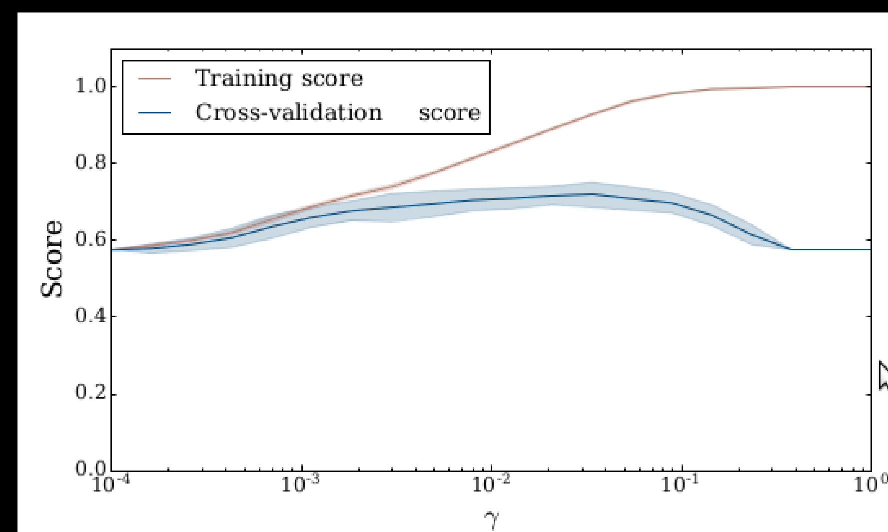

Results

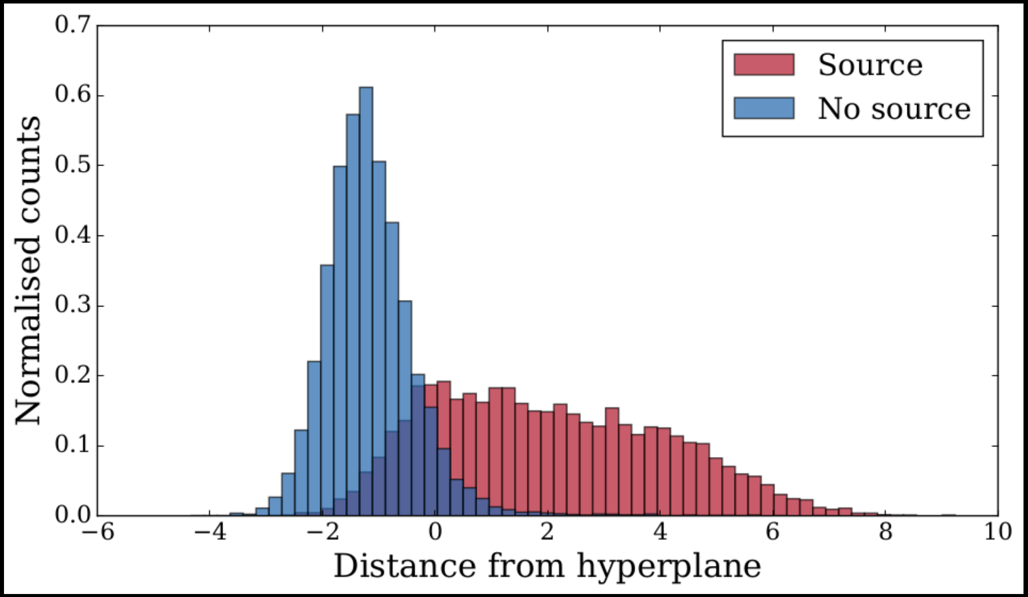

Raw score from SVM

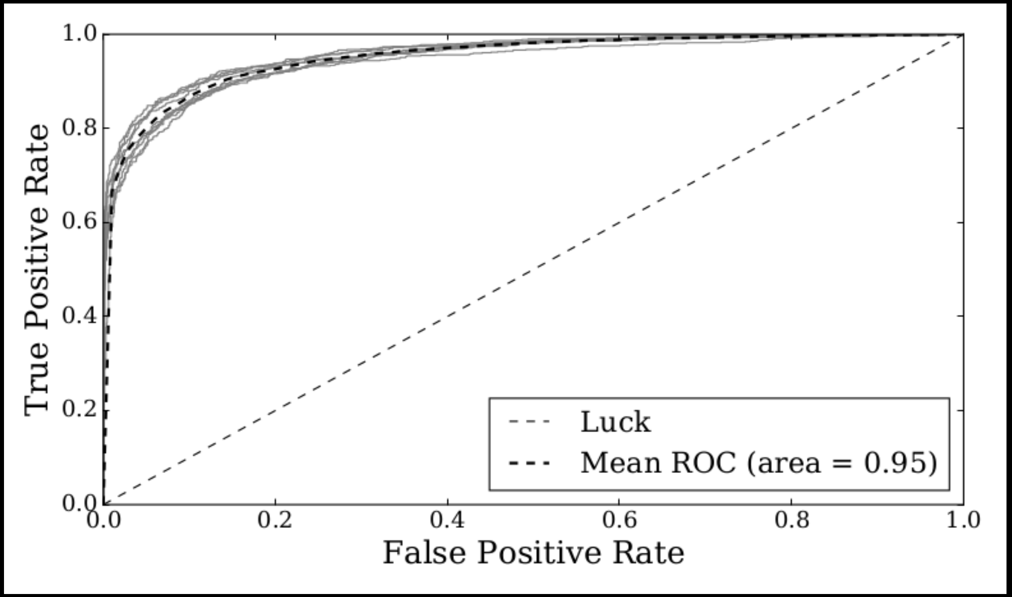

Receiver operating characteristic (ROC) curve

Results: Platt scaling

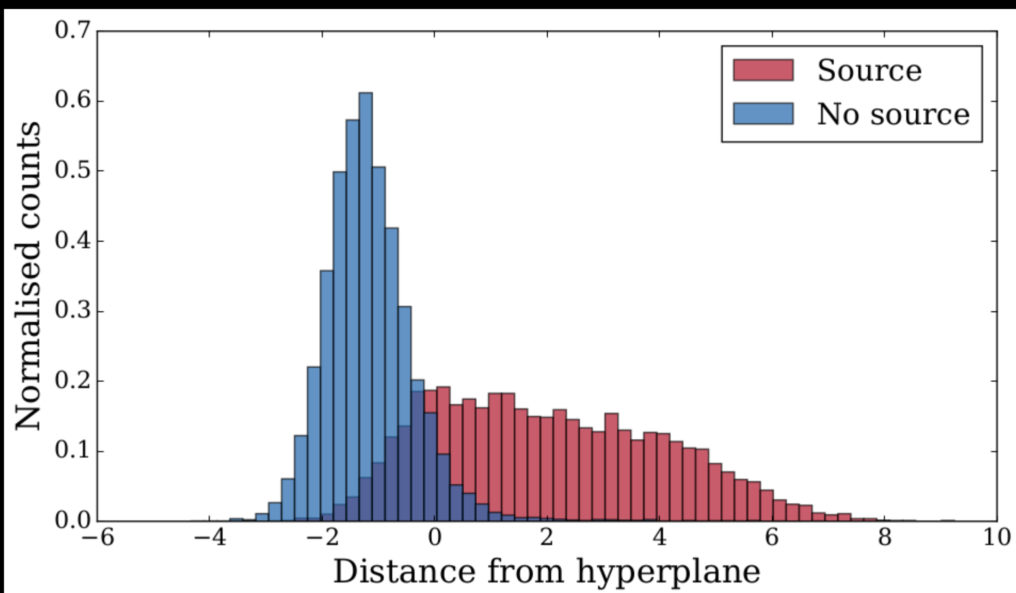

Raw score from SVM

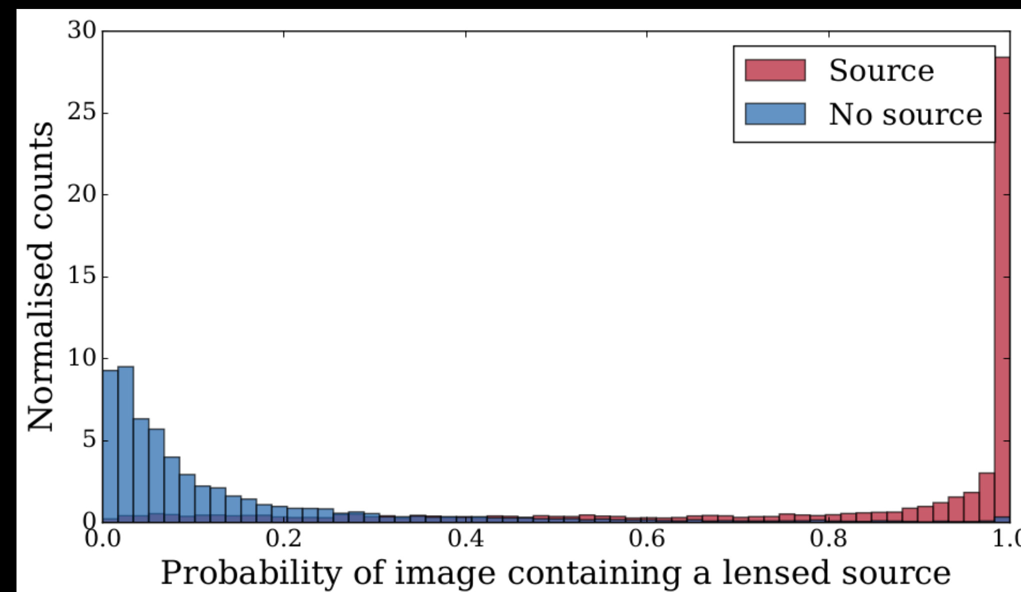

Convert output into calibrated probabilities

The University of Manchester

Lens Finding Challenge

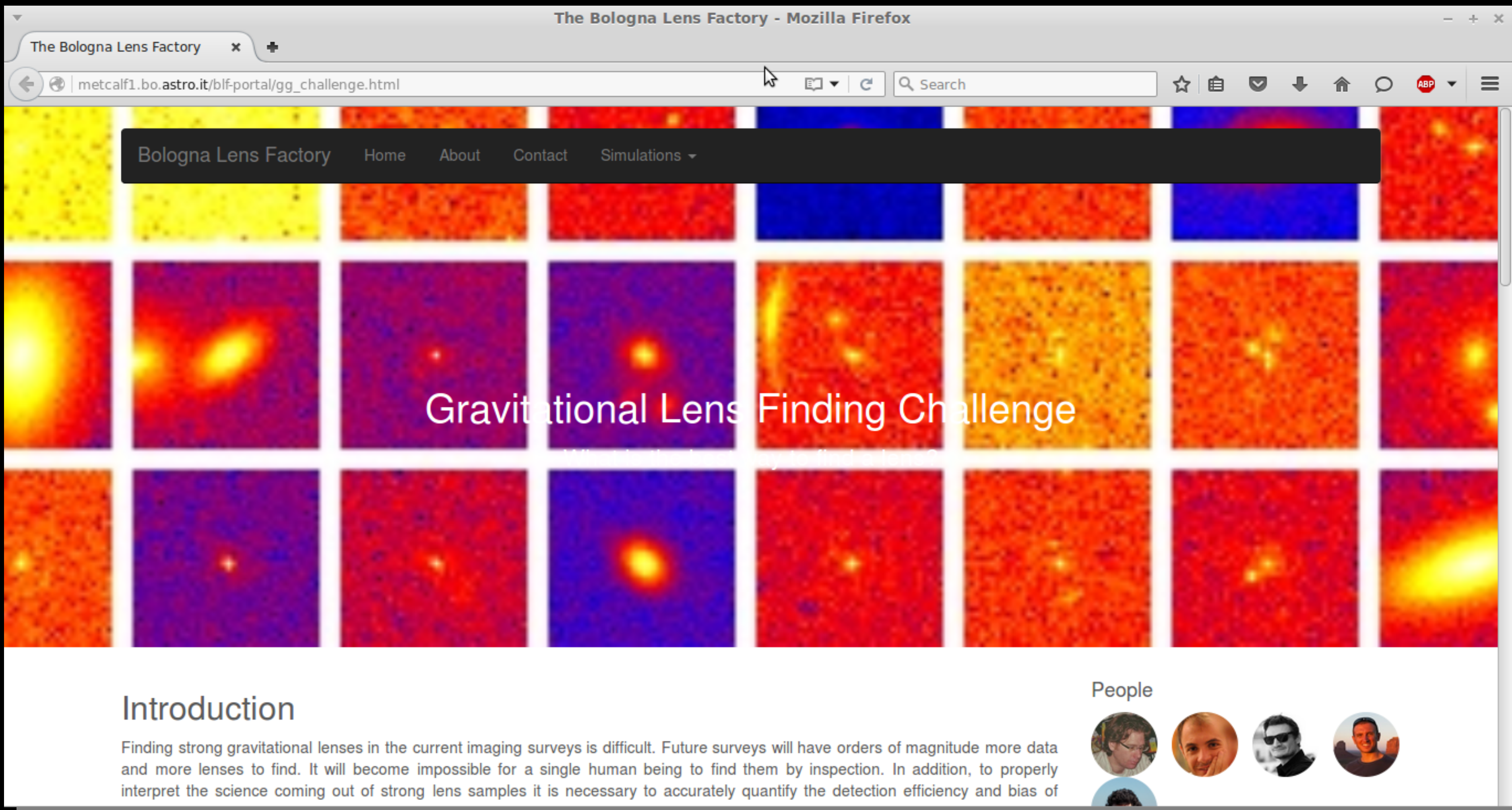

Metcalf et al., in preparation 2017

Machine vs human

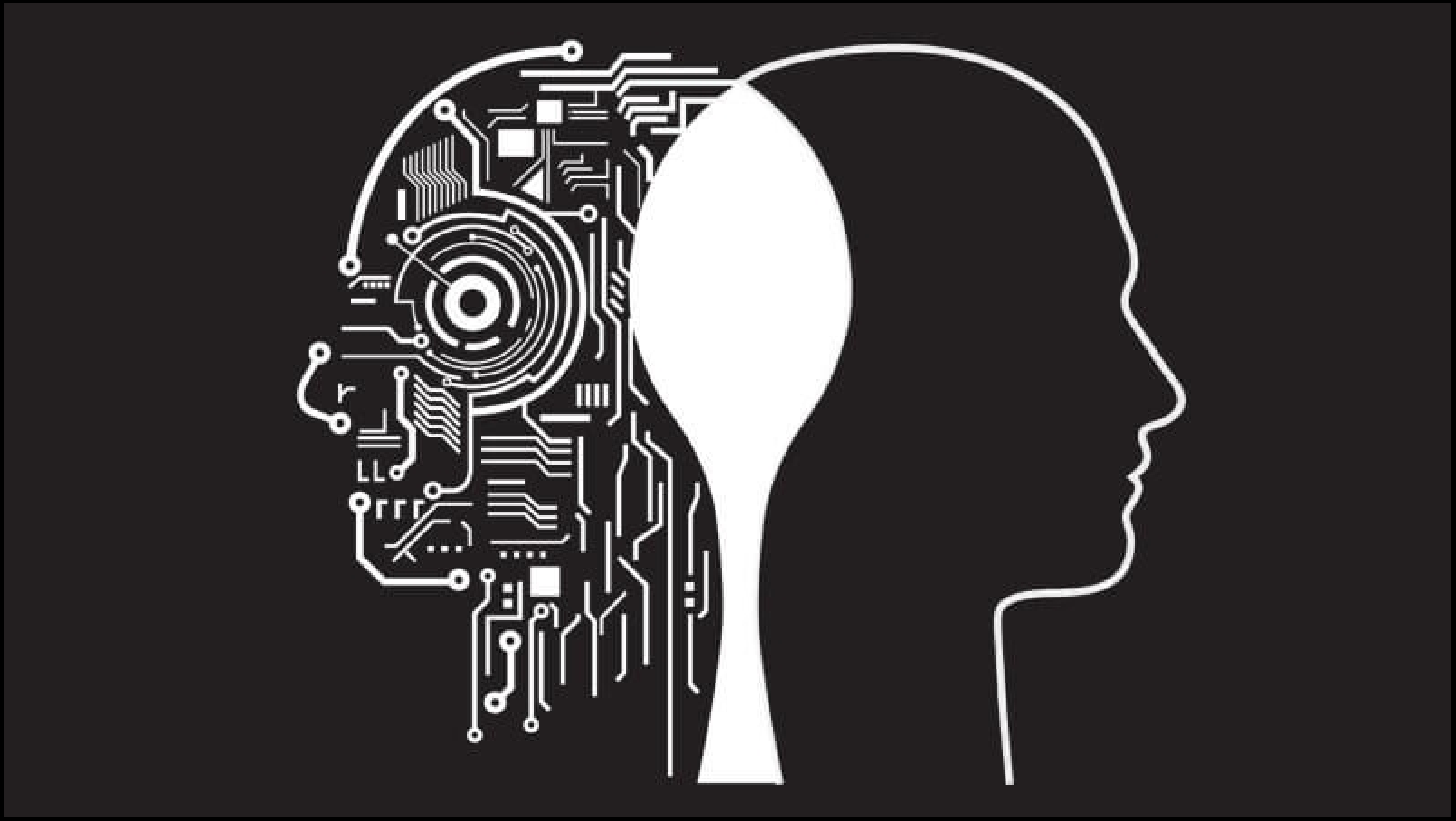

100 000 simulated images, 48 hours

MANCHESTER 1824
The University of Manchester

Lens Finding Challenge

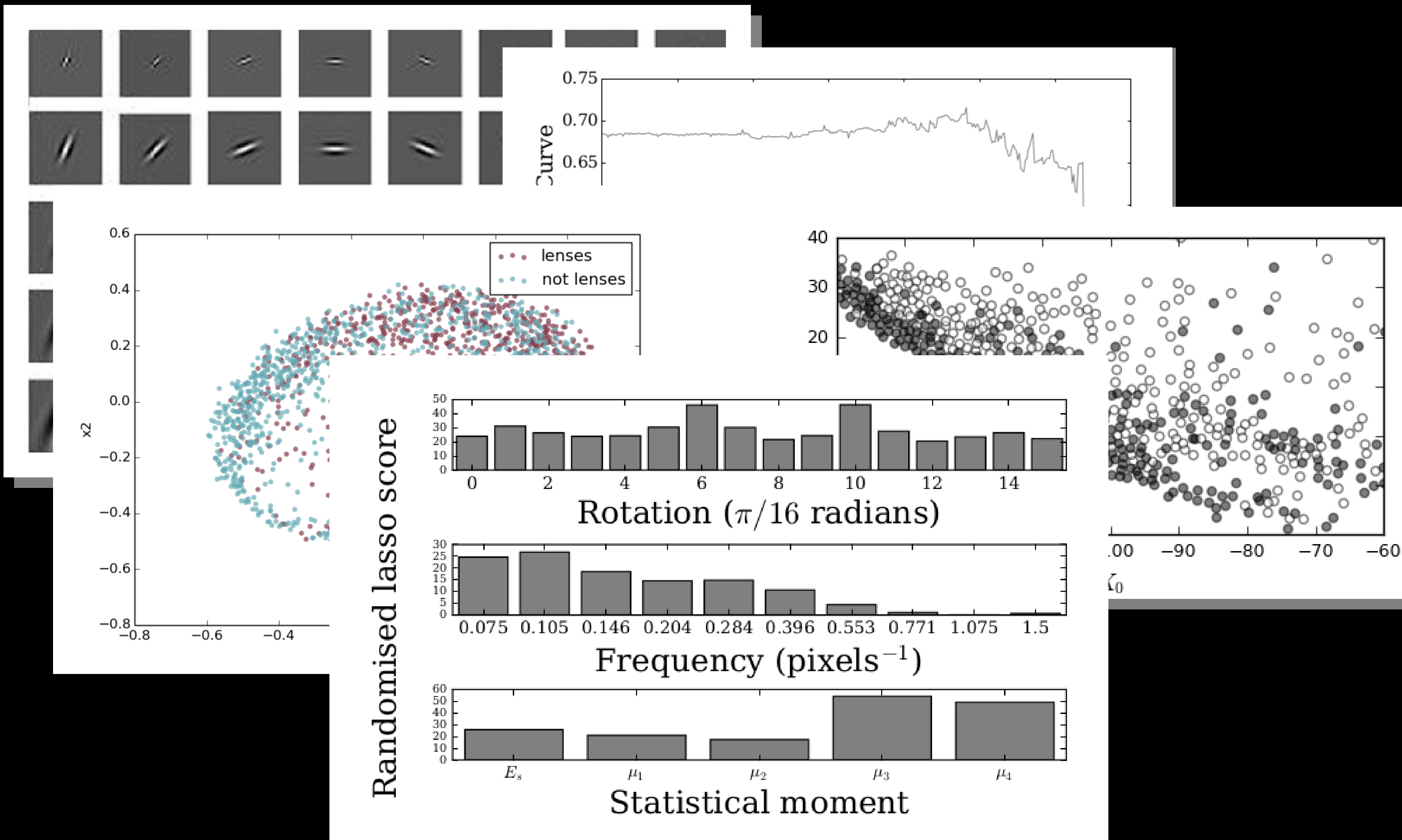

Lens Finding Challenge

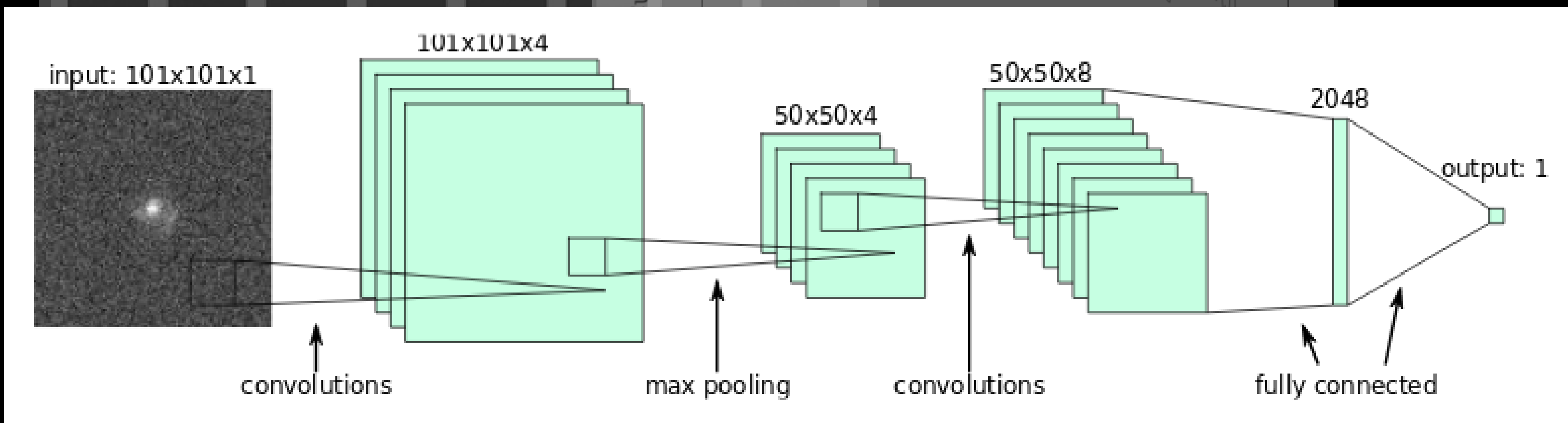

Convolutional neural network
Credit: Schaefer et al. 2017

Lens Finding Challenge

Credit: Schaefer et al. 2017

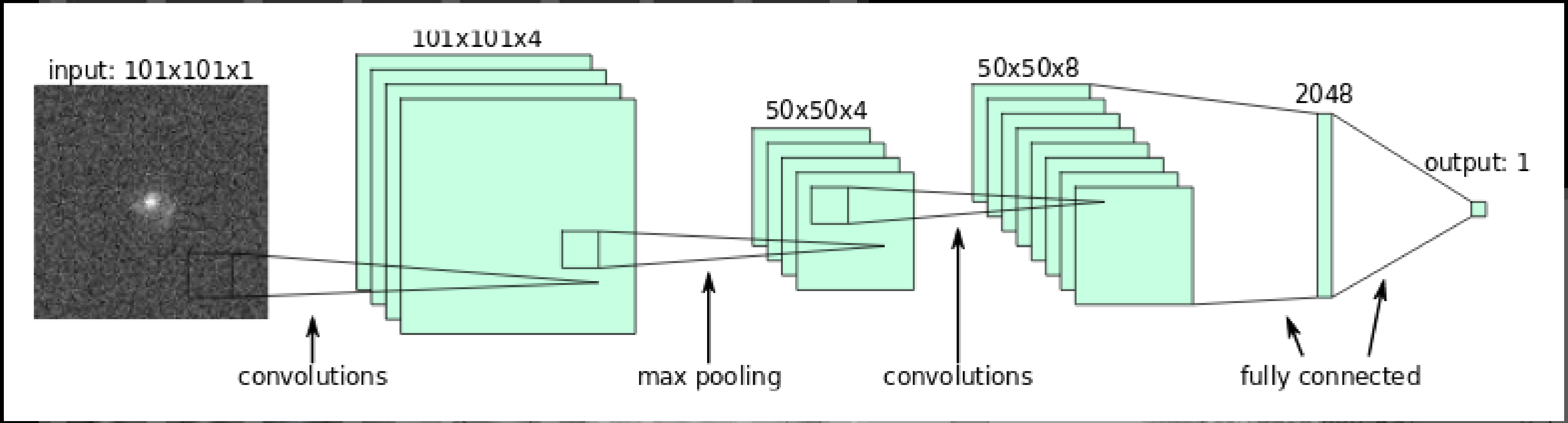

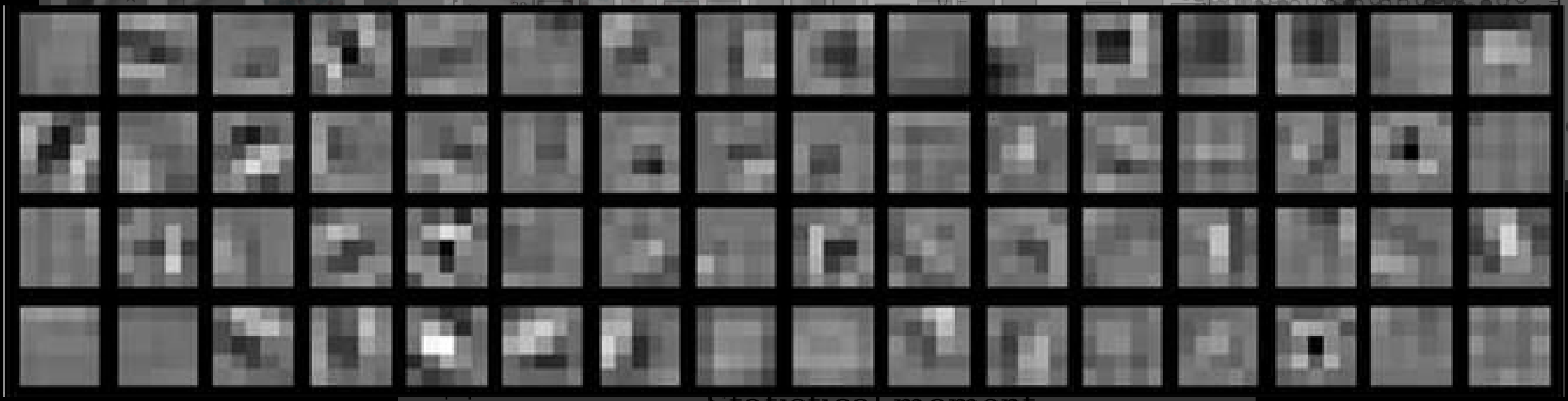

Lens Finding Challenge: results

Name	type	AUROC	TPR_0	TPR_{10}	short description
CMU-DeepLens-ResNet-ground3	Ground-Based	0.98	0.09	0.45	CNN
CMU-DeepLens-Resnet-Voting	Ground-Based	0.98	0.02	0.10	CNN
LASTRO EPFL	Ground-Based	0.97	0.07	0.11	CNN
CAS Swinburne Melb	Ground-Based	0.96	0.02	0.08	CNN
AstrOmatic	Ground-Based	0.96	0.00	0.01	CNN
Manchester SVM	Ground-Based	0.93	0.22	0.35	SVM / Gabor
Manchester-NA2	Ground-Based	0.89	0.00	0.01	Human Inspection
ALL-star	Ground-Based	0.84	0.01	0.02	edges/gradiants and Logistic Reg.
CAST	Ground-Based	0.83	0.00	0.00	CNN / SVM
YattaLensLite	Ground-Based	0.82	0.00	0.00	SExtractor

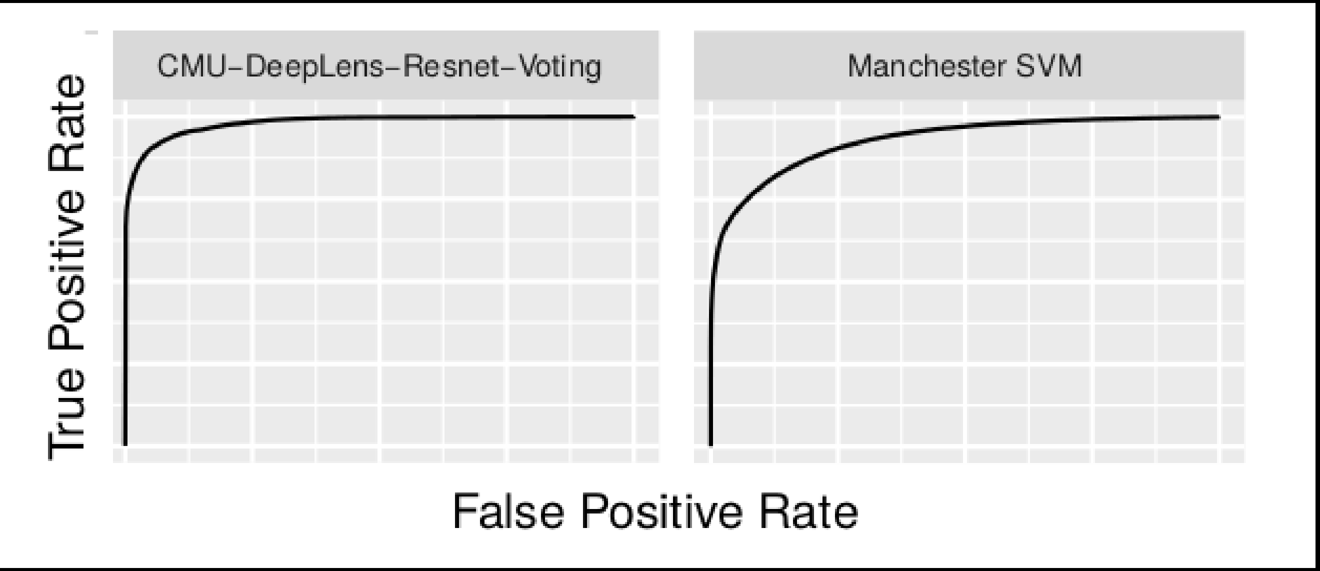

Metcalf et al., in preparation 2017

Lens Finding Challenge: results

Name	type	AUROC	TPR_0	TPR_{10}	short description
Manchester SVM	Ground-Based	0.93	0.22	0.35	SVM / Gabor
CMU-DeepLens-ResNet-ground3	Ground-Based	0.98	0.09	0.45	CNN
LASTRO EPFL	Ground-Based	0.97	0.07	0.11	CNN
CMU-DeepLens-Resnet-Voting	Ground-Based	0.98	0.02	0.10	CNN
CAS Swinburne Melb	Ground-Based	0.96	0.02	0.08	CNN
ALL-star	Ground-Based	0.84	0.01	0.02	edges/gradiants and Logistic Reg.
Manchester-NA2	Ground-Based	0.89	0.00	0.01	Human Inspection
YattaLensLite	Ground-Based	0.82	0.00	0.00	SExtractor
CAST	Ground-Based	0.83	0.00	0.00	CNN / SVM
AstrOmatic	Ground-Based	0.96	0.00	0.01	CNN

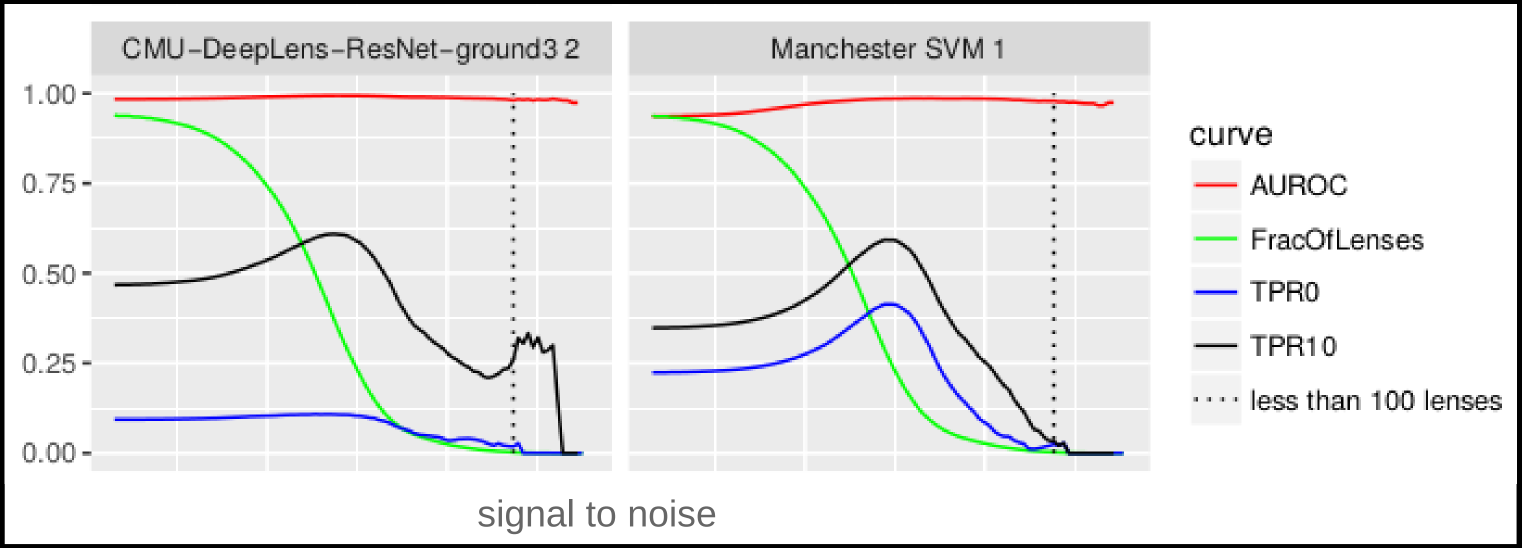

Metcalf et al., in preparation 2017

Real life data: Kilo Degree Survey

Domain adaptation

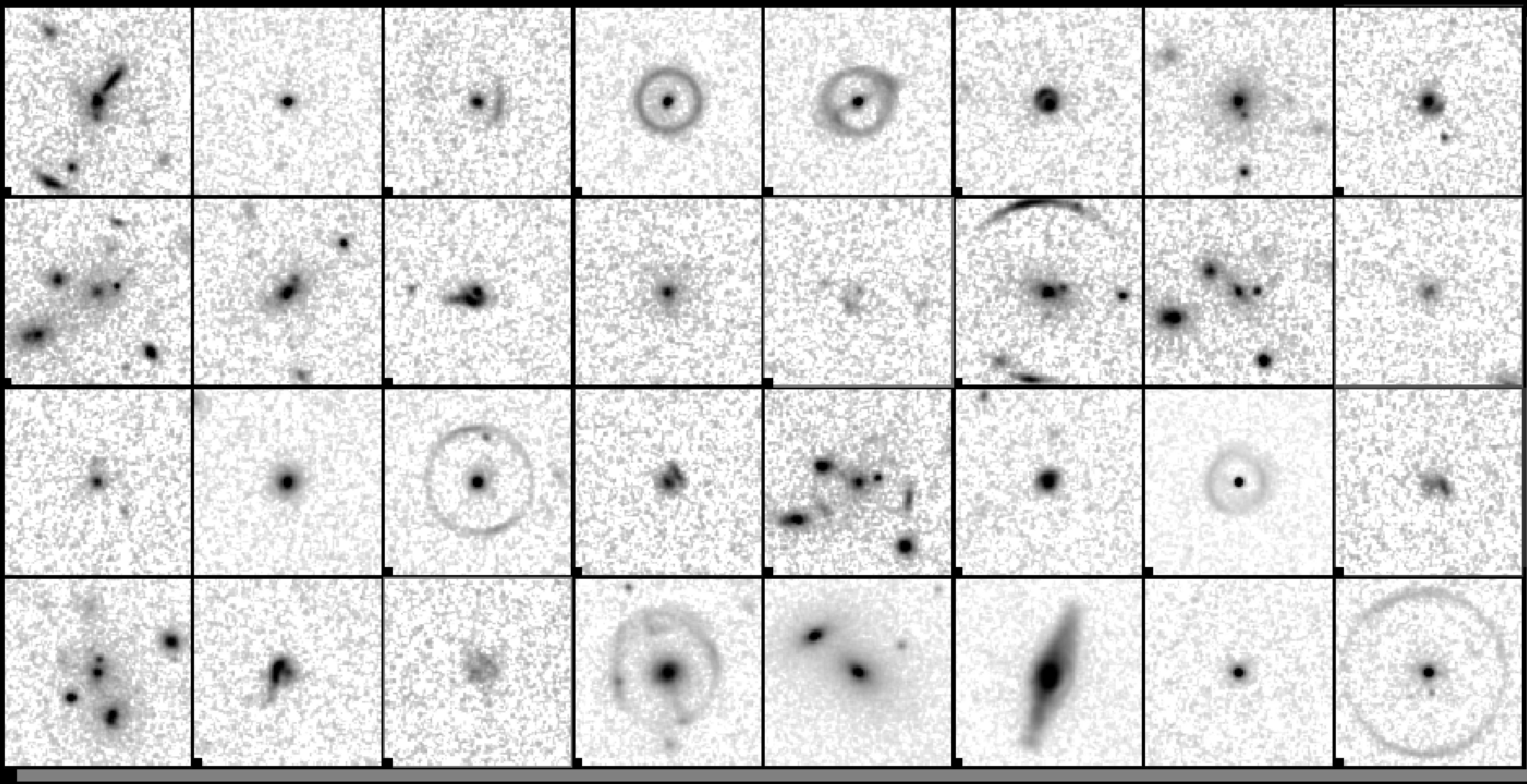

Real data: Kilo Degree Survey

1 000 000 real images after pre-selection

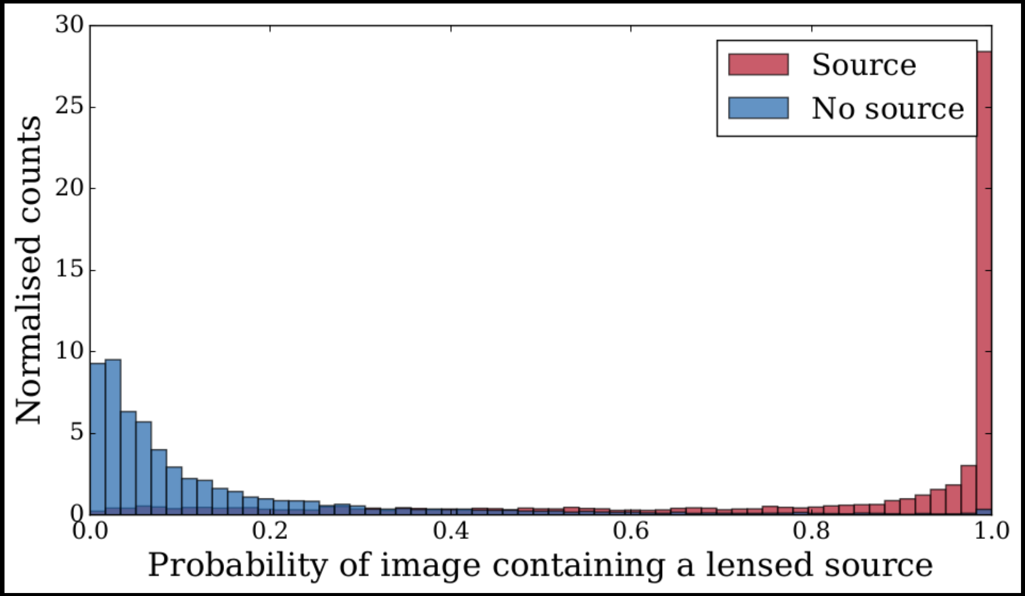

Classification of test mock data

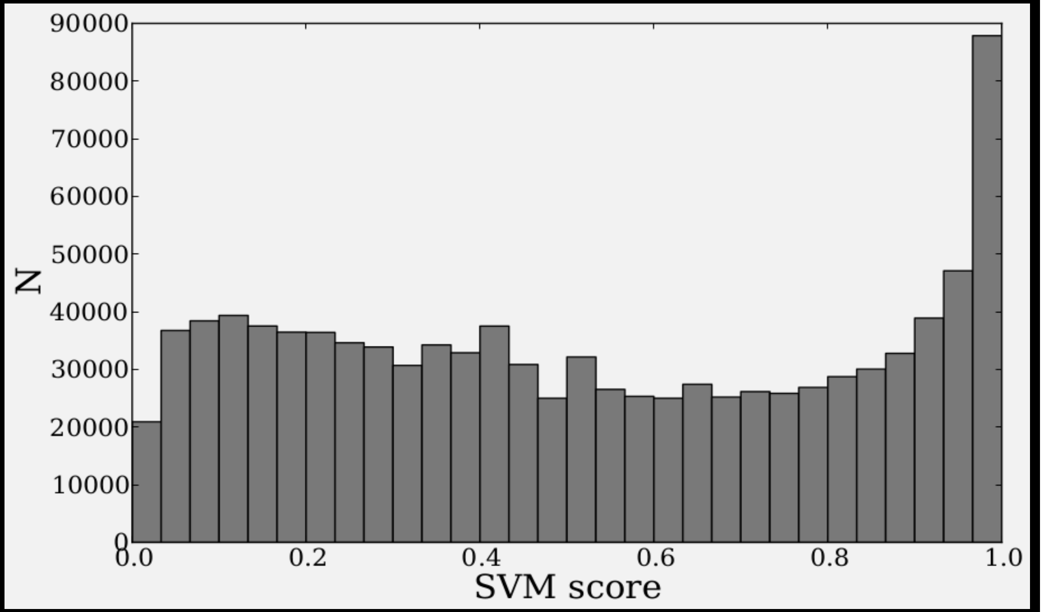

Classification of KiDS real data

Real life data: Kilo Degree Survey

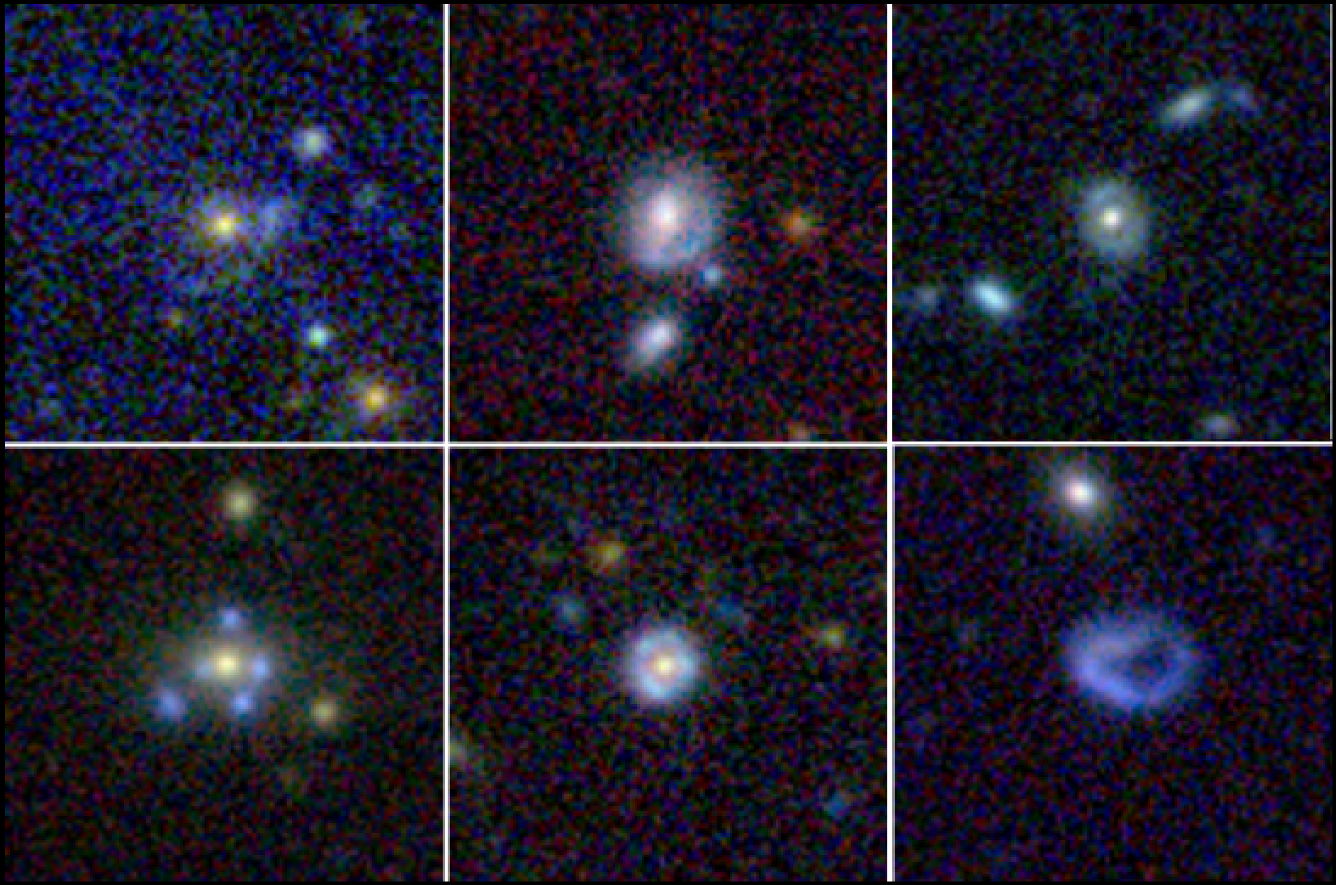

Hartley et al. 2017 MNRAS

Conclusions

- More lenses needed in order to exploit full scientific potential
- Machines now surpass humans in finding lenses
- Surprising strength of SVMs when false postives are a problem
- Domain adaption: limited by quality of training data
- The best architecture might be: CNN + SVM

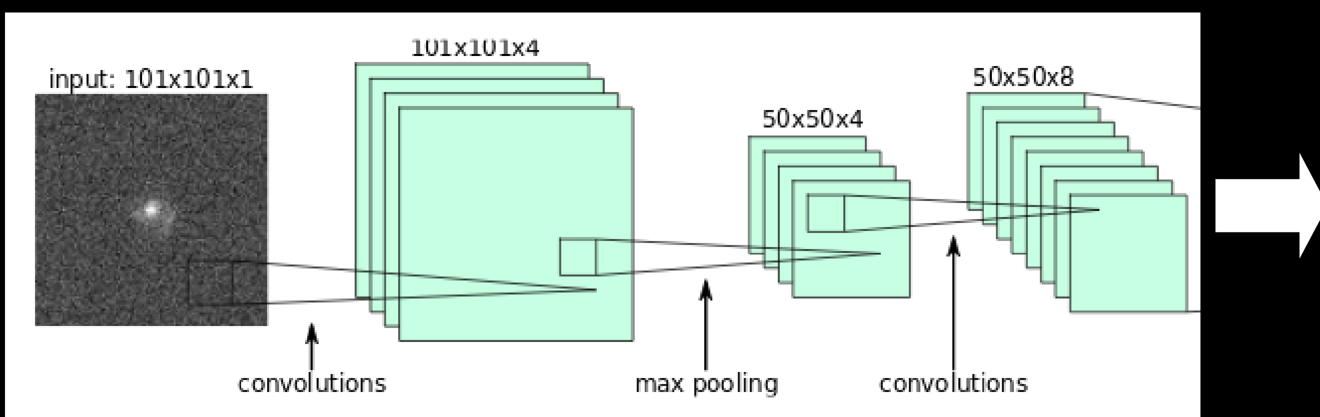

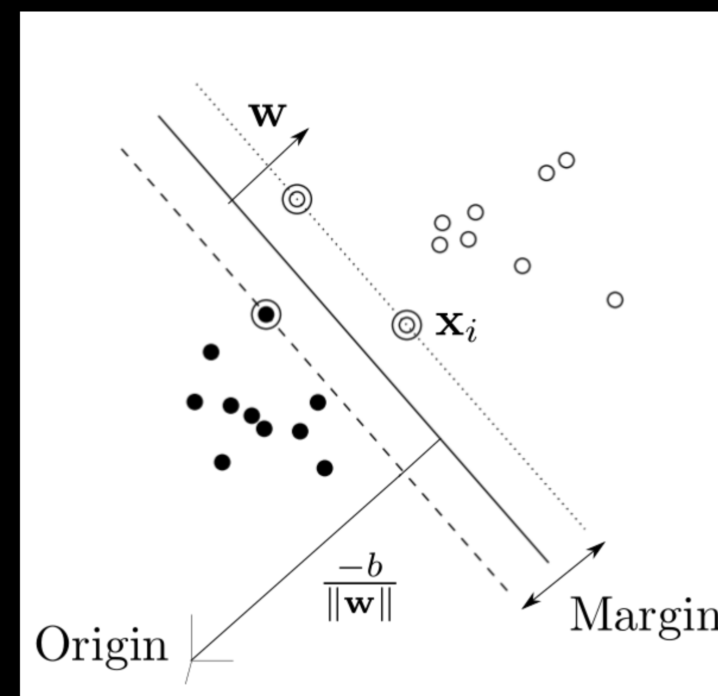

P. Hartley, R. Flamary, N. Jackson, A. S. Tagore, R. B. Metcalfe, MNRAS 471 (3): 3378-3397, 2017

Tuesday Dec 19th 2017, Laboratoire Lagrange, Université Côte d'Azur